Cerebral Cortex Advance Access published October 15, 2016

OXFORD

Cerebral Cortex, 2016; 1–19

doi: 10.1093/cercor/bhw304
Original Article

ORIGINAL ARTICLE

Temporal Evolution of Target Representation, Movement Direction Planning, and Reach Execution in Occipital–Parietal–Frontal Cortex: An fMRI Study

David C. Cappadocia[1,2,3], Simona Monaco[4], Ying Chen[1,2,3], Gunnar Blohm[5,6], and J. Douglas Crawford[1,2,3,6,7]

[1]Centre for Vision Research, York University, Toronto, ON, Canada, [2]School of Kinesiology and Health Science, York University, Toronto, ON, Canada, [3]Neuroscience Graduate Diploma Program, York University, Toronto, ON, Canada, [4]Center for Mind/Brain Sciences, University of Trento, Trento, Italy, [5]Centre for Neuroscience Studies, Queen's University, Kingston, ON, Canada, [6]Brain in Action CREATE / IRTG Program, Toronto, ON, Canada, and [7]Departments of Biology and Psychology, York University, Toronto, ON, Canada

Address correspondence to J. D. Crawford, York University, Centre for Vision Research, 0009A Lassonde Building, 4700 Keele Street, Toronto, ON M3J 1P3, Canada. Email: jdc@yorku.ca

Abstract

The cortical mechanisms for reach have been studied extensively, but directionally selective mechanisms for visuospatial target memory, movement planning, and movement execution have not been clearly differentiated in the human. We used an event-related fMRI design with a visuospatial memory delay, followed by a pro-/anti-reach instruction, a planning delay, and finally a "go" instruction for movement. This sequence yielded temporally separable preparatory responses that expanded from modest parieto-frontal activation for visual target memory to broad occipital–parietal–frontal activation during planning and execution. Using the pro/anti instruction to differentiate visual and motor directional selectivity during planning, we found that one occipital area showed contralateral "visual" selectivity, whereas a broad constellation of left hemisphere occipital, parietal, and frontal areas showed contralateral "movement" selectivity. Temporal analysis of these areas through the entire memory-planning sequence revealed early visual selectivity in most areas, followed by movement selectivity in most areas, with all areas showing a stereotypical visuo-movement transition. Cross-correlation of these spatial parameters through time revealed separate spatiotemporally correlated modules for visual input, motor output, and visuo-movement transformations that spanned occipital, parietal, and frontal cortex. These results demonstrate a highly distributed occipital–parietal–frontal reach network involved in the transformation of retrospective sensory information into prospective movement plans.

Key words: fMRI, movement planning, reach, visual memory, visuomotor transformations

Introduction

In order to effectively interact with the world, human beings take in sensory information and use it to produce meaningful actions. One of the most commonly studied cases of this is visually-guided reach-to-touch movements (e.g., ringing a doorbell or pushing the power button on a laptop computer). Often visual information is no longer available by the time one makes a movement, or gaze has been re-directed to another location by the time one initiates a movement (Henriques et al. 1998; Flanagan and Johansson 2003). To perform such

movements, the brain must retain information about the spatial location of a target in working memory, use this information to form a motor plan, and then execute that motor plan to reach towards the goal. Neurophysiological studies in awake behaving nonhuman primates have shown a progression from visual-to-motor (visuomotor) coding within and between neurons in the occipital–parietal–frontal cortical axis (Picard and Strick 2001; Andersen and Buneo 2002; Gail and Andersen 2006; Cisek and Kalaska 2010; Westendorff et al. 2010; Kravitz et al. 2011), and spatially-selective networks for memory, attention, and planning that span parietal and frontal cortex (Berman and Colby 2009; Rawley and Constantinidis 2009). However, human imaging studies have not clearly differentiated spatial selectivity for reach plans in cerebral cortex from visuospatial target representation and/or movement execution (ME), or tracked visual and movement directional selectivity through the entire sequence of events leading up to reach execution.

Previous human neuroimaging studies investigating visual-to-movement (visuo-movement) transformations have identified several key regions in the parietal–frontal reach planning network. In parietal cortex, both the mIPS (DeSouza et al. 2000; Medendorp et al. 2003, 2005; Prado et al. 2005; Beurze et al. 2007, 2009, 2010; Fernandez-Rui et al. 2007; Tosoni et al. 2008; Filimon et al. 2009; Chen et al. 2014) and the superior parietal occipital cortex (SPOC) (Astafiev et al. 2003; Connolly et al. 2003; Prado et al. 2005; Fernandez-Ruiz et al. 2007; Tosoni et al. 2008; Beurze et al. 2009; Gallivan et al. 2009, 2011; Bernier and Grafton 2010; Cavina-Pratesi et al. 2010; Monaco et al. 2011; Chen et al. 2014) show activation related to reach planning and execution. These areas encode this information with a contralateral left–right topography (Beurze et al. 2007; Vesia et al. 2010; Vesia and Crawford 2012). In frontal cortex, human dorsal premotor cortex (PMd) also encodes pointing and reaching (Connolly et al. 2000, 2007; Astafiev et al. 2003; Prado et al. 2005; Beurze et al. 2007, 2009, 2010; Bernier and Grafton 2010, Bernier et al. 2012; Chen et al. 2014), as well as contralateral spatial selectivity (Beurze et al. 2007, 2009, 2010; Bernier et al. 2012; Chen et al. 2014).

An important question in vision–memory–motor transformations is whether spatial locations and reach plans are specified in visual or movement selective coordinates, i.e., whether sustained spatial activity codes retrospective sensory information or prospective motor plans (Curtis 2006). One strategy scientists have used to study this question is dissociating the visual target from the movement goal. Some studies have used anti-reaching tasks, where subjects view a target and must perform a reach in the opposite direction (Connolly et al. 2000; Chen et al. 2014; Gertz and Fiehler 2015). Using this type of paradigm, Chen et al. (2014) found contralateral visual coding in left occipital cortex during the target representation period and contralateral movement directional coding in parieto–frontal cortex during ME. In another study, contralateral movement directional coding was observed in the left precuneus (PCu) during movement planning (MP) (Gertz and Fiehler 2015). Fernandez-Ruiz et al. (2007) studied visual and movement selective coding using reversing prisms, which reverse the visual input such that a leftward reach target appears to be in the right visual field. They found that most regions in the left posterior parietal cortex encoded the visual direction of the goal during ME (with the exception of the angular gyrus (AG), which encoded the movement direction).

What all of these imaging studies lacked, leading to the current study, was a clear separation between target memory, MP, and ME for reach. Some fMRI studies have isolated reach planning from execution, but slow BOLD dynamics did not allow a distinction between visual target memory and MP (Connolly et al. 2000; Beurze et al. 2007, 2009; Fernandez-Ruiz et al. 2007). In other studies, target memory was separated from MP, but did not distinguish planning from execution (Connolly et al. 2000; Chen et al. 2014). Based on these studies, one might predict that parieto–frontal cortex should show contralateral directional tuning for reach plans, especially in the hemisphere contralateral to the hand (Connolly et al. 2003; Fernandez-Ruiz et al. 2007; Bernier et al. 2012; Gertz and Fiehler 2015). However, one cannot clearly differentiate this spatial tuning for planning from coding target direction (and/or ME signals), especially in occipital cortex that might show tuning for either visual direction or an imaginary goal. Further, one cannot track visual versus movement directional tuning through a separate sequence of visual memory, planning, and execution events, or use this information to construct functional networks of sensory, motor, and sensorimotor codes for reach.

The current study uses an event-related fMRI paradigm that explicitly separates visually-guided reaching into 3 phases in time (visual target representation (VTR), MP, and ME), by introducing a pro/anti-reach instruction between visual target memory and planning phases, and a "go signal" between planning and execution times. We used this paradigm in combination with a new way of spatially analyzing combined pro-/anti-reach data, to investigate 4 questions: 1) which brain areas are differentially activated for VTR, MP, and ME, 2) which of these areas show contralateral visual and/or movement direction specificity during the planning phase, 3) at what point in the target–planning–execution coding sequence does a visual-to-movement (visuo-movement) transformation occur within the cortical areas involved in reach, and 4) how are these visual, movement, and visuo-movement parameters temporally and spatially distributed through the cortical networks for reach in the human?

Methods

Participants

Twelve right-handed subjects (3 males, 9 females aged 20–36) were recruited from the York University community. We chose this number of subjects based on precedents set in similar studies of visuomotor control in healthy subjects (Cavina-Pratesi et al. 2010, Gallivan et al. 2011). The resulting dataset was sufficient to yield statistically significant results that survived corrections for multiple comparisons (see Results). All subjects had normal or corrected-to-normal vision and none of the subjects had any known neurological deficits. The York University Human Participants Review Sub-committee approved all techniques used in this study and all participants gave their informed consent prior to the experiment.

Experimental Stimuli and Apparatus

The experimental stimuli and apparatus were the same as the setup used in Chen et al. (2014). Visual stimuli consisted of optic fibers embedded into a custom-built board with adjustable tilt. The board was mounted atop a platform whose height was also adjustable (Fig. 1A). The platform was attached to the MRI scanner bed and placed over the abdomen of the subject. The height of the platform and tilt of the board were adjusted for each participant to ensure comfortable reaching movements. A translucent touchscreen (Keytec, 170 × 126 mm) was affixed on the board to record reach endpoints. An eye-tracking system (iView X) was used in conjunction with the MRI-

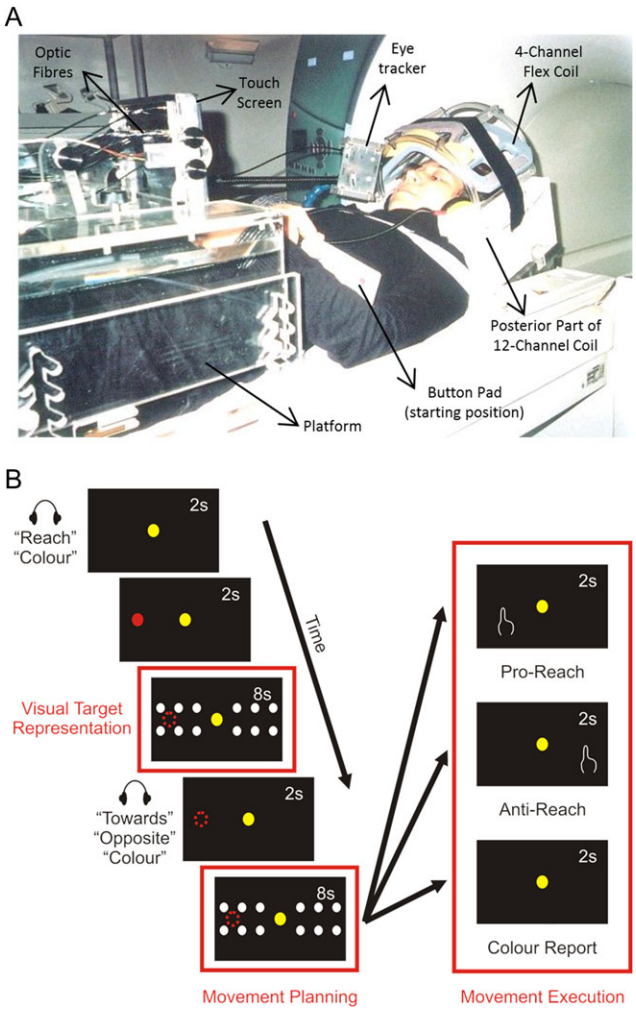

Figure 1. Experimental setup and paradigm. (*A*) Photograph of the experimental setup. (*B*) Illustration of the experimental paradigm. The display of visual targets is the same for all 3 tasks (Pro-Reach, Anti-Reach, and Color Report). The key difference between the 2 reach tasks is the congruence of the visual target and movement goal. In the Pro-Reach task, subjects reach towards the remembered location of the previously displayed visual target. In the Anti-Reach task, subjects reach towards the location mirror symmetrical to the visual target in the opposite visual field. As the target presentation and pro/anti instruction are separated by an 8 s delay, this allows the task to disentangle target representation from MP and execution. In the Color Report task, target color (red or green) rather than location is remembered and reported.

compatible Avotec Silent Vision system (RE-5701) to record movements of the right eye during the experiment.

The head of the participant was slightly tilted (~20°) to allow direct viewing of the stimuli presented on the board (Fig. 1A). The board was approximately perpendicular to gaze and approximately 60 cm from the eyes. The upper arm was strapped to the scanner bed to limit motion artifacts. Reaches were thus performed by movements of the right forearm and hand. A button pad was placed on the left side of the participants' abdomen and served as both the starting point for each trial and as the response for the color report control task (see Experimental Paradigm and Timing). Participants wore headphones to hear auditory instructions and cues. During each trial, subjects were in complete darkness with the exception of the visual stimuli, which were not bright enough to illuminate the workspace. The hand was never visible to the subject, even during reaching.

There were 3 types of visual stimuli presented by different colors: the fixation point in yellow, targets in green or red, and masks in white. All stimuli were presented horizontally on the touchscreen, and had the same diameter of 3 mm as the optic fibers. There was one central fixation location. Eight horizontal peripheral targets (4 on each side of the touchscreen) were used (Fig. 1B), and twenty "mask" LEDs were located above and below the target line (10 on each side with 5 above and 5 below the targets). The visual mask was used during the delay periods to control for visual afterimages. The distance between the eyes of the subject and the center of the touchscreen was approximately 60 cm. The target LEDs were located approximately 4°, 5°, 6°, or 7° to the left or right of the fixation LED.

Experimental Paradigm and Timing

We used an event-related design, with each trial lasting 38 s (including an inter-trial interval of 12 s). The paradigm included 3 tasks: pro-reach, anti-reach, and color report as a control (Fig. 1B). Each trial began with the presentation of the yellow fixation LED (this was displayed for 24 s before the first trial in each run). Concurrently, subjects were given the auditory instruction "reach" or "color" to indicate the task they had to perform at the end of that trial. The important distinction between these 2 instructions is that while remembering the spatial location of the target LED (the visual target) was required for the reaching trials, this information could be ignored for the color report trials. After 2 s, a green or red target LED was illuminated for 2 s, followed by an 8-s delay period (the "visual target representation" phase) during which the fixation LED and mask LEDs were illuminated. At the end of the delay, subjects were given 1 of 3 auditory instructions: For reach trials: "towards" (indicating a pro-reach trial) or "opposite" (indicating an anti-reach trial). For color report trials the instruction "color" was repeated. This took 2 s. The pro- or anti-reach instruction being given in the middle of the trial prevented subjects from forming their movement plan during the first delay period. The auditory instruction was followed by another 8-s delay period (the "movement planning" phase) during which the fixation LED and mask LEDs were illuminated. After the mask LEDs were turned off, subjects heard a beep that served as a "go" signal for subjects to reach-to-touch to: 1) the remembered location of the target in pro-reach trials, 2) the mirror location in the opposite visual hemifield in anti-reach trials, or 3) press the button once if the target LED was green or twice if it was red for the color report trials (or vice versa, this was be counterbalanced across subjects). This is referred to as the "movement execution" phase. After touching the touchscreen for 2 s, subjects heard a beep that instructed them to return their right index finger to the starting position. The following trial started 12 s later.

Each functional run consisted of 12 trials presented in a random order (4 for each of the 3 tasks; 50% of targets presented in each visual hemifield for each task) and lasted about 8 min. For the purpose of analysis, target locations were collapsed together as "left" or "right." Subjects participated in 8 functional runs in one session. They were trained to perform the required tasks 1–2 days before imaging and practiced all tasks within the MRI scanner before scanning to ensure that they were comfortable with the task.

Behavioral Recordings

Following the fMRI experiments, the eye position and reach endpoints were inspected. Eye movement errors were defined as trials where subjects were unable to maintain visual fixation from target presentation until touching the touchscreen. Reaching errors were defined as reaches to the direction opposite to the instructed reach goal. Trials with behavioral errors were excluded from further analysis (4.52% of trials).

To confirm accurate reaching in the pro- and anti-reach conditions, we performed a correlation analysis comparing horizontal target location to the horizontal reach endpoint for each subject. For pro-reach trials, across-subject means of the correlation coefficients (r) were $r = 0.843 \pm 0.03$. For anti-reach trials, across-subject means of the correlation coefficients were $r = 0.836 \pm 0.04$. We then applied Fischer's r-to-z transformations to individual subject's r values and performed one-way t-tests to compare subjects' z scores to 0. Both t-tests were significant ($P_{pro} < 0.001$, $P_{anti} < 0.001$), indicating accurate reaching.

Imaging Parameters

The experiment was conducted at the York MRI Facility at the Sherman Health Sciences Centre at York University with a 3-T whole-body MRI system (Siemens Magnetom TIM Trio). The posterior half of a 12-channel head coil (6 channels) was placed at the back of the head, with a 4-channel flex coil over the anterior part of the head (Fig. 1A). The head was tilted ~20° to allow for direct viewing of the stimuli during experimental trials.

Functional data was acquired using an echo-planar imaging sequence (repetition time [TR] = 2000 ms; echo time [TE] = 30 ms; flip angle [FA] = 90°; field of view [FOV] = 192 × 192 mm, matrix size = 64 × 64 leading to an in-slice resolution of 3 × 3 mm; slice thickness = 3.5 mm, no gap; 36 transverse slices angled at ~25° covering the whole brain). Slices were collected in ascending and interleaved order. During each experimental session, a T1-weighted anatomical reference volume was acquired using an MPRAGE sequence (TR = 1900 ms; TE = 2.52 ms; inversion time TI = 900 ms; FA = 90°; FOV = 256 × 256 × 192 mm, voxel size = 1 × 1 × 1 mm^3).

Preprocessing

All data was analyzed using BrainVoyager QX 2.2 (Brain Innovation). The first 2 volumes of each scan were discarded to avoid T1 saturation effects. For each run, slice scan time correction (cubic spline), temporal filtering (removing frequencies <2 cycles/run), and 3D motion correction (trilinear/sinc) were performed. The 3D motion correction was performed by aligning each volume of one run to the volume of the functional scan that was closest in time to the anatomical scan. Three runs showing abrupt head movement of 1 mm or 1° were discarded. Functional runs were coregistered to the anatomical image. Functional data was then transformed into Talairach space using the spatial transformation parameters from each individual subject's anatomical scan. The voxel size of the native functional images was 3 × 3 × 3 and was not resampled to a different voxel size during the preprocessing steps. Functional data was spatially smoothed using a FWHM of 8 mm.

Data Analysis

For each participant, we used a general linear model with 33 predictors. Two predictors were used for the initial auditory instruction (reach or color); 4 predictors were used for visual target presentation (left or right X reach or color trial); 4 predictors were used for VTR (left or right X reach or color trial); 3 predictors were used for the second auditory instruction (pro-reach, anti-reach, or color trial); 6 predictors were used for motor preparation (left or right X pro-reach, anti-reach, or color trial); 6 predictors were used for motor execution (left or right X pro-reach, anti-reach, or color trial). In addition, 6 motion correction parameters and predictors for behavioral errors and inter-trial intervals were added as confound errors. Each predictor was derived from a rectangular wave function convolved with a standard hemodynamic response function using BrainVoyager QX's default double-gamma hemodynamic response function.

Voxelwise Analysis

Contrasts were performed on β weights using an RFX (random effects) GLM with a percentage signal change transformation. This GLM was used to investigate the first 2 main questions for this study. To investigate the brain areas involved in VTR, reach MP, and reach ME, we performed 3 contrasts to find brain areas that showed higher activity for reach trials (pro and anti) than the control (color) trials during each phase.

We also performed 2 contrasts to test if brain areas showed contralateral directionally selective activation in visual or movement direction coordinates during MP. The first contrast was designed to find contralateral visually selective brain areas. So for the left hemisphere, areas that showed higher activation when the target was initially presented in the right visual field (pro- and anti-reach right) than the left (pro- and anti-reach left) would be contralaterally visually selective. For the right hemisphere, areas that showed higher activation when the target was initially presented in the left visual field (pro- and anti-reach left) than the right (pro- and anti-reach right) would be contralaterally visually selective. The other contrast aimed at finding movement-direction selective brain areas. So for the left hemisphere, areas that showed higher activation when the movement direction was to the right (pro-reach right and anti-reach left) than the left (pro-reach left and anti-reach right) would be contralaterally movement selective. For the right hemisphere, these areas showed higher activation when the movement direction was to the left (pro-reach left and anti-reach right) than the right (pro-reach right and anti-reach left). For these contrasts, we limited our analysis to brain regions showing higher BOLD activation in the hemisphere contralateral to the visual target or movement goal, respectively.

Activation maps for group voxelwise results were overlaid on the inflated brain of one representative subject. To correct for multiple comparisons, cluster threshold corrections (Forman et al. 1995) were performed for each contrast using BrainVoyager QX's cluster-level statistical threshold estimator plug-in (1000 iterations). Areas that did not survive were excluded from further analysis. A Bonferroni correction was applied to the t value for each contrast to account for the 2 types of contrasts performed in the experiment (movement trials > control trials and contralateral directional selectivity contrasts). These 2 types of contrasts were planned a priori, with contrasts 1–3 being movement > control trials at 3 different time periods and contrasts 4 & 5 investigating contralateral visual and movement selectivity during the planning phase ($\alpha = 0.05/2$ comparisons = 0.025 corrected for $P < 0.05$).

Results

General Reach Activation for VTR, MP, and ME for Reach

In our first analysis, we looked at general, nondirectional reach activation; combining left and right movements for both pro- and anti-reach trials. A recent fMRI study has shown that pro- and anti-reaches activate similar parietal and premotor areas (Gertz and Fiehler 2015). We confirmed this was the case in our study by analyzing pro-reach > color, anti-reach > color, and pro-reach > anti-reach during motor planning and execution and have included these post hoc analyses in Supplementary Fig. 1. As indicated in this figure, most of the ROIs described below fall within regions of pro-/anti-reach overlap, although some additional significant ROIs appear below when one doubles the dataset by combining these 2 conditions.

Figure 2A–C plot the pro- and anti-reach data relative to our color control task in each of the 3 major phases of our task: VTR, MP, and ME, with corresponding ß-weights for these data shown in Supplementary Fig. 2, and the corresponding Talairach coordinates shown in Tables 1–3. Brain areas were labeled by comparing the Talariach coordinates from the peak voxel within a cluster and comparing it to known sites of activation in the visuomotor system. It is important to note that certain effector-specific functional areas cannot be clearly distinguished in our contrasts (e.g., frontal eye fields vs. PMd), in which case the reach-related label has been given. We also provided complete time series data for select areas (Fig. 3). These data are described in more detail in the following sections.

Task Related Activation During the Visual Target Representation Phase

Contrast 1 [Target Representation Reach > Target Representation Color] investigated which brain areas showed higher activation for visuospatial coding required to plan a reach (either pro or anti) than activation related to representing the color of the target (the requirement of the control task). In this phase, only the visual target location was known (as reach direction was only specified by an auditory instruction after this delay period), and any activation revealed by this contrast may be related to any aspect of target coding (not limited to spatial location). Figure 2A shows the activation map for this contrast superimposed on inflated cortical surfaces viewed from above. The indicated areas survived a cluster threshold correction of 82 voxels. This contrast revealed modest bilateral activation near the intersection of the precentral and

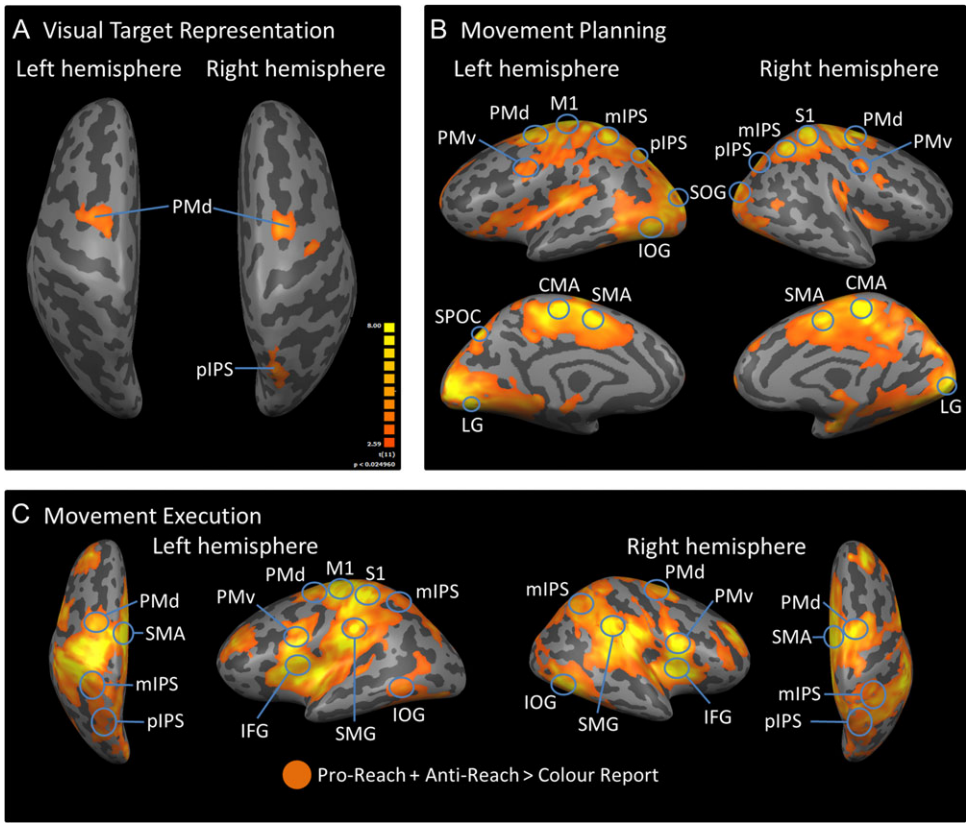

Figure 2. (A) Voxelwise statistical maps obtained from the RFX GLM for the contrast Pro-Reach + Anti-Reach > Color report. Event-related group activation maps for target representation are displayed on the "inflated brain" of one representative subject, where light gray represents gyri and dark gray represents sulci. The leftward inflated brain represents the left hemisphere, and the rightward brain represents the right hemisphere. Highlighted areas show significantly higher activation than control data with a $P < 0.05$ with Bonferroni and cluster threshold corrections. These areas include the left and right PMd and right pIPS. (B) Voxelwise statistical maps obtained from the RFX GLM for the contrast Pro-Reach + Anti-Reach > Color report. Event-related group activation maps are displayed on the inflated brain of one representative subject for MP. The 2 leftward inflated brains represent the left hemisphere, and the 2 rightward brains represent the right hemisphere. Highlighted areas show significantly higher activation than control data with a $P < 0.05$ with Bonferroni and cluster threshold corrections. These areas include bilateral PMd, PMv, mIPS, pIPS, and SOG. Significant activation was also observed in left M1, SPOC, and IOG, and right S1. (C) Voxelwise statistical maps obtained from the RFX GLM for the contrast Pro-Reach + Anti-Reach > Color report. Event-related group activation maps are displayed on the inflated brain of one representative subject for ME. The 2 leftward inflated brains represent the left hemisphere, and the 2 rightward brains represent the right hemisphere. Highlighted areas show significantly higher activation than control data with a $P < 0.05$ with Bonferroni and cluster threshold corrections. These areas include bilateral PMd, mIPS, SMG, IOG, SMA, and IFG. Significant activation was also observed in left M1 and S1, and in right PMv. (See Table 4 for site abbreviations).

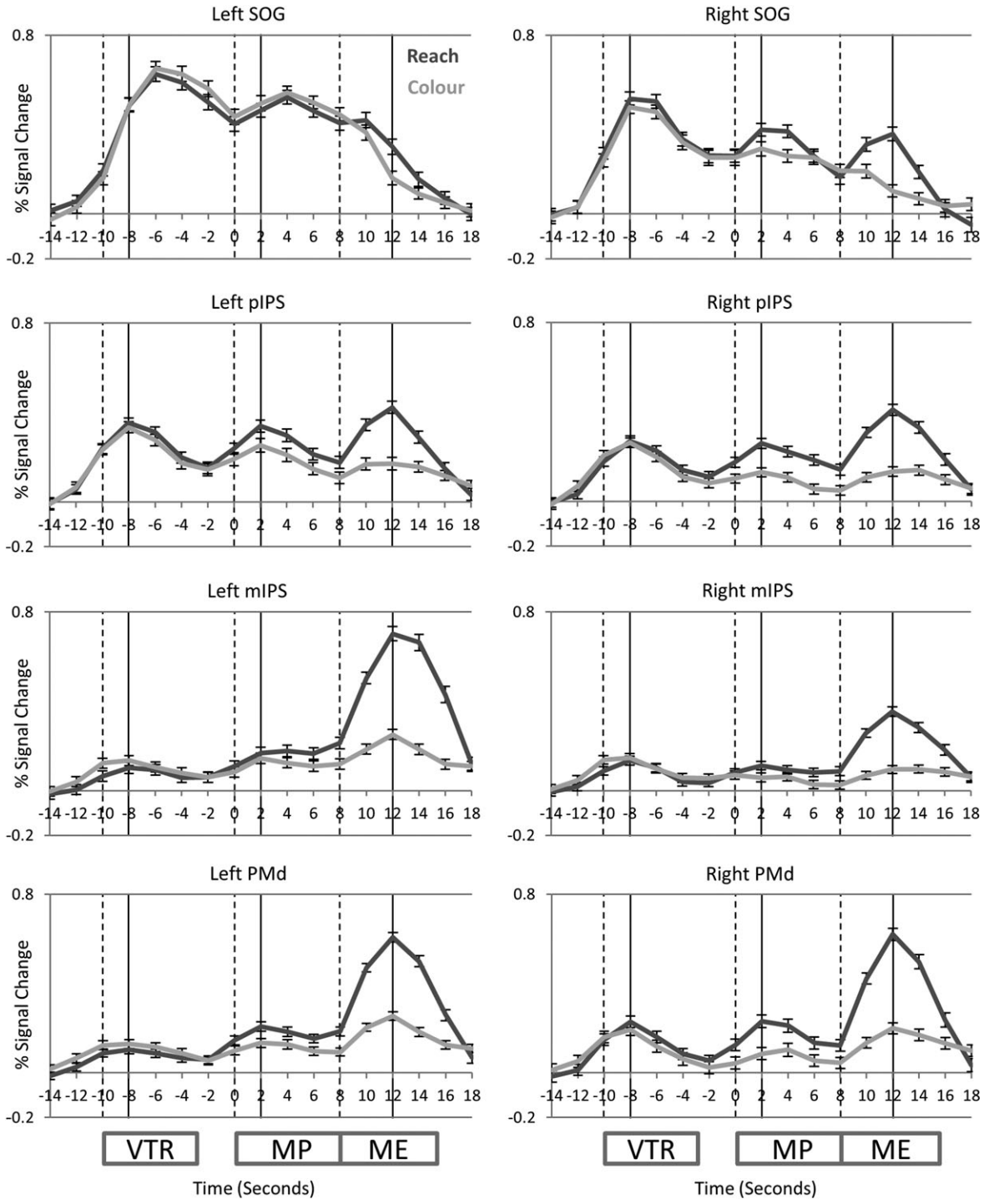

Figure 3. Time courses for 4 brain areas of interest (SOG, pIPS, mIPS, and PMd) that were bilaterally active from the MP Reach (pro + anti) > MP Color contrast during the MP phase. The dark gray line indicates activity (% signal change) from reach trials and the light gray line indicates activity from color report trials. Error bars are SEM across subjects. The *x*-axis displays time in seconds and is time locked to the MP phase. The 3 vertical black dashed lines indicate the onset of the VTR, MP, and ME phases (from left to right). Note that there is an activation peak corresponding to the black solid lines for all 7 time courses that contain 3 peaks (B-H), the only exception being left SOG.

superior frontal sulci, consistent with the location of PMd (Monaco et al. 2011), and modest unilateral activation in the right posterior intraparietal sulcus (pIPS). At first glance it might seem odd that only areas associated with movement control (Gallivan and Culham 2015) were activated, but recall that the control task also involves memory of a non-spatial, non-motor target type. Thus, this subtraction shows areas with memory-epoch activity "specific to spatial location or early general motor preparation for reach."

Task Related Activation During the MP Phase

Contrast 2 [MP Reach (pro + anti) > MP Color] investigated which brain areas showed higher activation for MP for pro- or

Table 1. Talairach coordinates and number of voxels for Target Representation ROI

Area	Mean X	Mean Y	Mean Z	Voxels
Left PMd	−25.43	−10.48	52.47	976
Right PMd	20.61	−9.4	51.53	976
Right pIPS	21.64	−61.84	48.21	909

Table 2. Talairach coordinates and number of voxels for MP ROI

Area	Mean X	Mean Y	Mean Z	Voxels
Left SOG	−13.47	−89.31	14.38	959
Right SOG	24.31	−79.24	26.31	935
Left IOG	−44.32	−79.63	−0.47	696
Left LG	−10.5	−77.5	−12.5	1000
Right LG	7.5	−74.5	−12.5	1000
Left mIPS	−24.5	−44.5	52.5	1000
Right mIPS	22.5	−46.5	44.5	1000
Left pIPS	−18.5	−68.5	38.5	1000
Right pIPS	18.5	−59.5	45.5	1000
Left SPOC	−22.41	−73.51	32.58	979
Left PMd	−15.5	−14.5	58.5	1000
Right PMd	23.5	−14.5	56.5	1000
Left PMv	−51.47	−5.51	34.47	964
Right PMv	45.51	−2.53	31.44	964
Left CMA	−7.5	−23.5	49.5	1000
Right CMA	8.5	−26.5	48.5	1000
Left SMA	−7.5	−9.5	54.5	1000
Right SMA	10.5	−4.5	45.5	1000
Right S1	16.5	−34.5	58.5	1000
Left M1	−15.51	−26.49	61.49	997

Table 3. Talairach coordinates and number of voxels for ME ROI

Area	Mean X	Mean Y	Mean Z	Voxels
Left IOG	−51.42	−65.21	−4.27	722
Right IOG	46.5	−60.5	−7.5	1000
Left pIPS	−8.11	−65.31	51.09	582
Right pIPS	13.78	−70.79	46.53	579
Left mIPS	−24.5	−44.5	52.5	1000
Right mIPS	22.5	−46.5	44.5	1000
Left SMG	−52.5	−23.5	19.5	1000
Right SMG	52.5	−20.5	32.5	999
Left PMd	−25.6	−6.1	55.3	1000
Right PMd	23.5	−5.5	58.5	1000
Left PMv	30.46	42.46	31.46	990
Right PMv	−34.5	41.5	25.5	1000
Left IFG	−57.85	1.84	18.67	835
Right IFG	55.44	9.53	4.56	986
SMA	−4.5	−12.5	51.5	1000
Left S1	−25.5	−23.5	61.5	1000
Left M1	−20.5	−17.5	65.5	999

anti-reach than activation related to representing the color of the target (the requirement of the control task). Activation during this phase could be related to planning a specific movement and/or general motor preparation in anticipation of an upcoming reach. The activation map for this contrast is shown on an inflated cortical surface viewed from the lateral and medial sides (Fig. 2B). The marked areas survived a cluster threshold correction of 230 voxels. This contrast revealed widespread activation in bilateral PMd, ventral premotor cortex (PMv), supplementary motor area (SMA), cingulate motor area (CMA), mIPS, pIPS, superior occipital gyrus (SOG), lingual gyrus (LG). Activation was also found in the left hemisphere in primary motor cortex (M1), SPOC, and inferior occipital gyrus (IOG), and in right primary somatosensory cortex (S1). (For a complete list of abbreviations for ROI discussed in this study, see Table 4).

Task Related Activation During the ME Phase

Contrast 3 [ME Reach (pro + anti) > ME Color] investigated which brain areas showed higher activation related to executing a pro- or anti-reach than activation related to indicating the color of the target with a button press (the requirement of the control task). The activation map for this contrast is shown on an inflated cortical surface (Fig. 2C). The marked areas survived a cluster threshold correction of 206 voxels. This contrast revealed widespread activation in bilateral mIPS, M1, PMd, inferior frontal gyrus (IFG), supramarginal gyrus (SMG), and IOG. Activation was also found in the left hemisphere in primary somatosensory cortex (S1), in the right hemisphere in the middle frontal gyrus, and in the SMA (could not disentangle the right and left hemisphere for SMA).

Time Series Data

To better understand the evolution of activation for these brain areas, we examined their time series. Figure 3 illustrates the time courses data of the reach and color conditions for 4 representative bilateral brain areas, chosen because they have been linked to visuomotor planning, including: SOG, pIPS, mIPS, and PMd. We selected these areas as SOG showed egocentric planning-related activation in a previous study (Chen et al. 2014) and pIPS, mIPS, and PMd are part of the parieto–frontal reach planning network (Culham et al. 2006; Gallivan et al. 2011; Vesia and Crawford 2012). The onset time for VTR, MP, and ME are indicated by gray vertical lines (noting that the BOLD response data have been time-corrected for estimated hemodynamic lag), with black lines indicating peak values during these 3 phases from left to right, respectively.

Looking at these representative time courses, several patterns emerge that help to understand the previous observations and provide reference events for further analysis. First, in nearly all of our ROIs 3 peaks of activation were apparent, aligned closely with target representation, MP, and ME. An exception to this general trend was the lack of a distinctive third execution peak for some occipital areas, such as left SOG (Fig. 3) and bilateral LG (not shown). Second, the relative heights of these peaks were dependent on the expected functional anatomy, with SOG (representing occipital cortex) showing a relatively larger target peak (although "planning" and "execution" peaks were present in the right cortex), pIPS showing roughly equal target, planning, and execution peaks, and mIPS and PMd showing predominant ME peaks. Third, the degree of reach task-specificity (gap between black vs. gray lines) generally increased both in time from visual target representation to ME and in cortical space from occipital cortex to parietal cortex to frontal cortex. Thus, the entire occipital–parietal–frontal axis was activated during target coding, planning, and execution, but the task-specificity of these responses increased along the antero-frontal axis and in the temporal transition from target, planning, and execution responses. We will examine this in more detail in the following sections using spatial parameters related to visual target and movement direction.

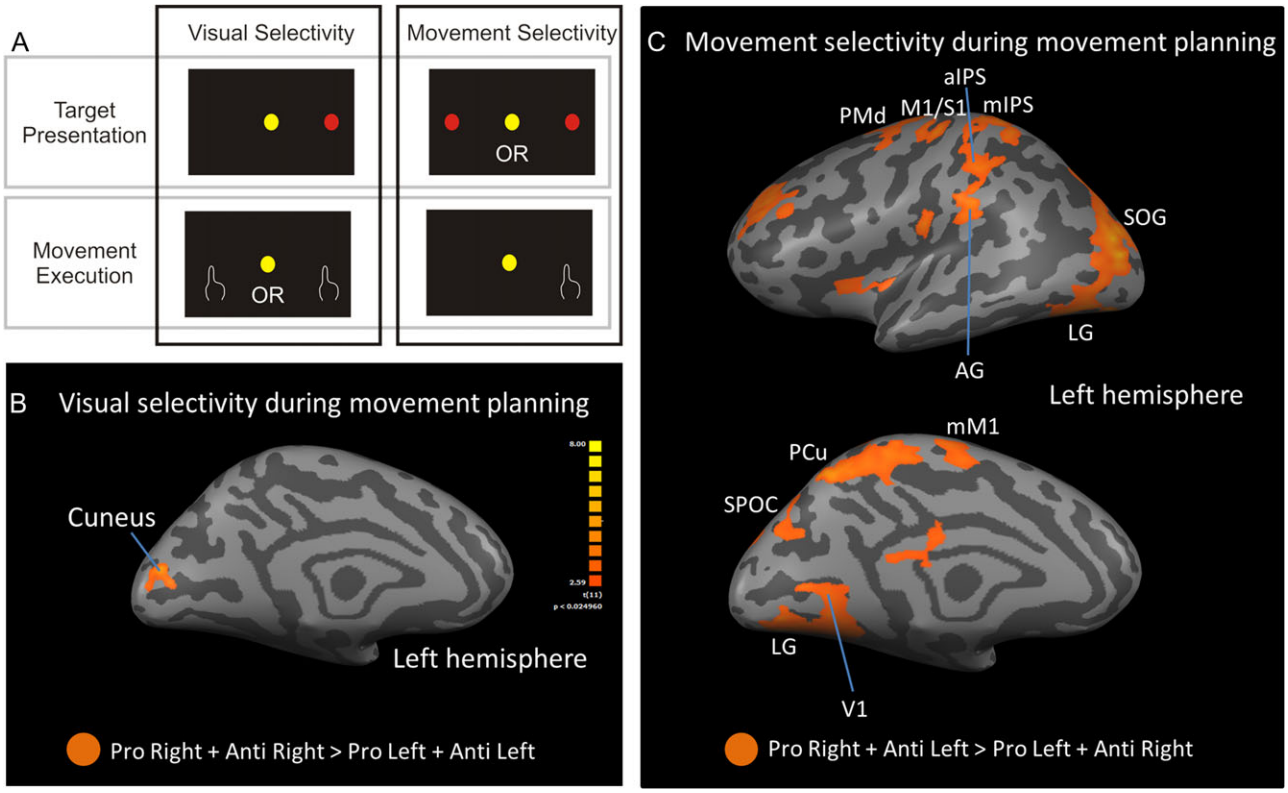

Figure 4. (*A*) A visualization of the visual target and movement goal selectivity contrasts used in this experiment. For the visual selectivity contrasts, trials where the target was initially presented in the right visual field were contrasted against trials where the visual target was presented to the left, independent of the direction of the movement. For movement selectivity contrasts, the opposite was the case. Trials where the motor goal was to the right were contrasted against trials where the motor goal was to the left, independent of where the initial visual target was presented. These contrasts were used to examine activity during the MP phase. (*B*) Voxelwise statistical maps obtained from the RFX GLM for the contrast Pro-Reach Right + Anti-Reach Right > Pro-Reach Left + Anti-Reach Left. Event-related group activation maps are displayed on the left hemisphere inflated brain of one representative subject for MP. Highlighted areas show significantly higher activation than control data with a $P < 0.05$ with Bonferroni and cluster threshold corrections. The Left cuneus met these criteria. (*C*) Voxelwise statistical maps obtained from the RFX GLM for the contrast Pro-Reach Right + Anti-Reach Left > Pro-Reach Left + Anti-Reach Right. Event-related group activation maps are displayed on the left hemisphere inflated brain of one representative subject for MP. Highlighted areas show significantly higher activation than control data with a $P < 0.05$ with Bonferroni and cluster threshold corrections. These areas include V1, LG, SOG, SPOC, mIPS, aIPS, PCu, AG, PMd, mM1, and an area encompassing parts of primary motor and somatosensory cortices (M1/S1) (See Table 4 for site abbreviations).

Contralateral Visual and Movement Direction Selectivity during MP

We next focused on the question of whether spatially selective activation during reach planning encodes retrospective visual location information and/or prospective movement information (Curtis 2006). Henceforth, we will refer to these as "visual" and "movement" direction selectivity, respectfully, for brevity. After the pro or anti instruction, participants might hypothetically still retain memory of target location (left or right), while simultaneously planning a movement in the same or opposite direction. We took advantage of this to create contrasts that utilized all of the planning data, and either highlighted 1) visual direction selectivity where the pro-/anti-movement selectivity should cancel out (as in the right-target example shown in the left column of Fig. 4A) or 2) movement direction selectivity, where left/right target direction should cancel out (as in the rightward movement example shown in the right column of Fig. 4A). We focused our analysis on contralateral activation given the breadth of evidence for this type of directional selectivity in previous studies (fMRI (Medendorp et al. 2003; 2005; Filimon et al. 2009; Vesia and Crawford 2012; Gertz and Fiehler 2015), MEG (Van Der Werf et al. 2010), TMS (Vesia et al. 2010), patients (Khan et al. 2007) and primate neurophysiology (Gail and Andersen 2006; Gail et al. 2009; Westendorff et al. 2010)). Consistent with some previous studies (Connolly et al. 2003; Fernandez-Ruiz et al. 2007; Bernier et al. 2012; Gertz and Fiehler 2015) we only found contralateral directional tuning in reach-related areas located within the left hemisphere (opposite to the reaching hand). These areas are shown in Figure 4B,C (with corresponding ß-weights provided in Supplementary Fig. 3 and Talairach coordinates in Table 5). Some other regions of ipsilateral sensitivity appeared in both hemispheres in regions not generally associated with reach; these were eliminated from further analysis.

Visual Direction Selectivity

Contrast 4 [(pro-reach right target + anti-reach right target) – (pro-reach left target + anti-reach left target)] investigated contralateral visual selectivity during the MP phase in the left hemisphere, as trials where the visual target was presented in the right visual field were contrasted from trials where the visual target was presented to the left, regardless of the movement goal. The marked areas survived a cluster threshold correction of 75 voxels. In this contrast, the left cuneus was the only area to show significant contralateral activation for visual target

Table 4. List of ROI brain area abbreviations

Area	Abbreviation
Occipital	
Primary visual cortex	V1
Lingual gyrus	LG
Superior occipital gyrus	SOG
Inferior occipital gyrus	IOG
Parietal	
Superior parietal occipital cortex	SPOC
Posterior intraparietal sulcus	pIPS
Midposterior intraparietal sulcus	mIPS
Anterior intraparietal sulcus	aIPS
Angular gyrus	AG
Supramarginal gyrus	SMG
Precuneus	PCu
Primary somatosensory cortex	S1
Frontal	
Primary moror cortex	M1
Dorsal premotor cortex	PMd
Ventral premotor cortex	PMv
Cingulate motor area	CMA
Supplementary motor area	SMA
Inferior frontal gyrus	IFG

Table 5. Talairach coordinates and number of voxels for contralateral visually and motor selective areas during MP in the left hemisphere

Area	Mean X	Mean Y	Mean Z	Voxels
Visually selective				
Cuneus	−2.56	−77.12	14.67	691
Motor selective				
V1	−7.46	−76.05	−0.52	798
SOG	−28.51	−83.51	15.51	998
LG	−21.44	−74.43	−14.49	985
mIPS	−25.36	−45.39	58.35	961
SPOC	−24.6	−73.82	35.33	716
aIPS	−33.58	−27.39	50.78	902
Pcu	−4.46	−62.81	49.69	767
AG	−60.91	−36.32	24.07	823
PMd	−25.61	−3.38	58.67	671
mM1	−4.22	−17.19	63.32	859
M1/S1	−30.38	−16.12	56.13	891

direction (Fig. 4*B*). A similar contrast was performed on the right hemisphere [(pro-reach left target + anti-reach left target) – (pro-reach right target + anti-reach right target)] but failed to yield significant activation that met our localizer criteria.

Movement Direction Selectivity

Contrast 5 [(pro-reach right target + anti-reach left target) – (pro-reach left target + anti-reach right target)] investigated contralateral movement selectivity during the MP phase in the left hemisphere, as trials where the movement goal was to the right were contrasted from trials where the movement goal was to the left, regardless of the initial visual presentation. The marked areas survived a cluster threshold correction of 149 voxels. This contrast revealed widespread contralateral movement selectivity in occipital, parietal, and frontal areas (Fig. 4*C*), including primary visual cortex (V1), LG, SOG, SPOC, mIPS, anterior intraparietal sulcus (aIPS), PCu, AG, PMd, medial primary motor cortex (mM1), and an area bordering on primary motor and somatosensory cortex (M1/S1). This illustrates a network of reach-associated areas concerned with specifying upcoming reach direction during the planning phase. A similar contrast was performed on the right hemisphere [(pro-reach left target + anti-reach right target) – (pro-reach right target + anti-reach left target)] but failed to yield significant activation that met our localizer criteria.

Temporal Evolution of Visual and Movement Direction Coding

One of the main aims of our visual and movement direction selective voxelwise contrasts were to localize established reach-related regions for a more detailed temporal analysis on their time course data. This allowed us to understand the time course of visual and motor selectivity both within and across cortical sites. In these analyses, we traced the entire time course of visual and movement selectivity in the areas shown in Figure 4 using both the visual direction contrast (contrast 4) and the movement direction contrast (contrast 5). We also did the same for 4 sites in the left hemisphere obtained independently from the analysis in Figure 2, and obtained nearly identical results (Supplementary Fig. 4).

Time Courses of Visual and Movement Direction Selectivity

Figure 5 plots the time courses of the visual directional selectivity (black lines) and movement directional selectivity (gray lines) for every region identified in Figure 4, with the exception of aIPS which showed relatively flat responses and is associated more with grasp than reach transport (Culham et al. 2006). As all of these regions are in the left hemisphere, visual direction selectivity was calculated by subtracting the time courses for trials where the visual target was presented ipsilaterally (pro-reach left and anti-reach left) from trials where the visual target was presented contralaterally (pro-reach right and anti-reach right). Movement direction selectivity for these areas was calculated by subtracting the time courses for trials with an ipsilateral reach (pro-reach left and anti-reach right) from trials with a contralateral reach (pro-reach right and anti-reach left). Supplementary Figs. 5–7 show the time courses for these component signals, including % signal change for visual direction-selective activation for pro-reach left + anti-reach left, and pro-reach right + anti-reach right, as well as movement-selective activation for pro-reach left + anti-reach right and pro-reach right + anti-reach left.

Returning to Figure 5, one-sample *t*-tests were performed to compare the % BOLD signal change at the time of the peak visual and motor activation to zero to indicate significant directional tuning in either the visual or motor domain (○). We limited our comparisons to these 2 points in time to indicate the presence of visual or movement direction selectivity in a brain area without needing to correct for multiple comparisons across all time points. As there were 2 *t*-tests, we performed a Bonferroni correction for 2 comparisons ($\alpha = 0.05/2$ comparisons = 0.025 corrected for $P < 0.05$). Our occipital, parietal, and frontal areas are divided into 3 columns for easier comparison, with "early" to "late" areas organized top to bottom. Again, several trends emerge from this time-course analysis. First, whereas reach general activation followed 3 peaks of event-related responses (Fig. 3), directional selectivity showed only 2 peaks: the first a visual peak aligned with target presentation,

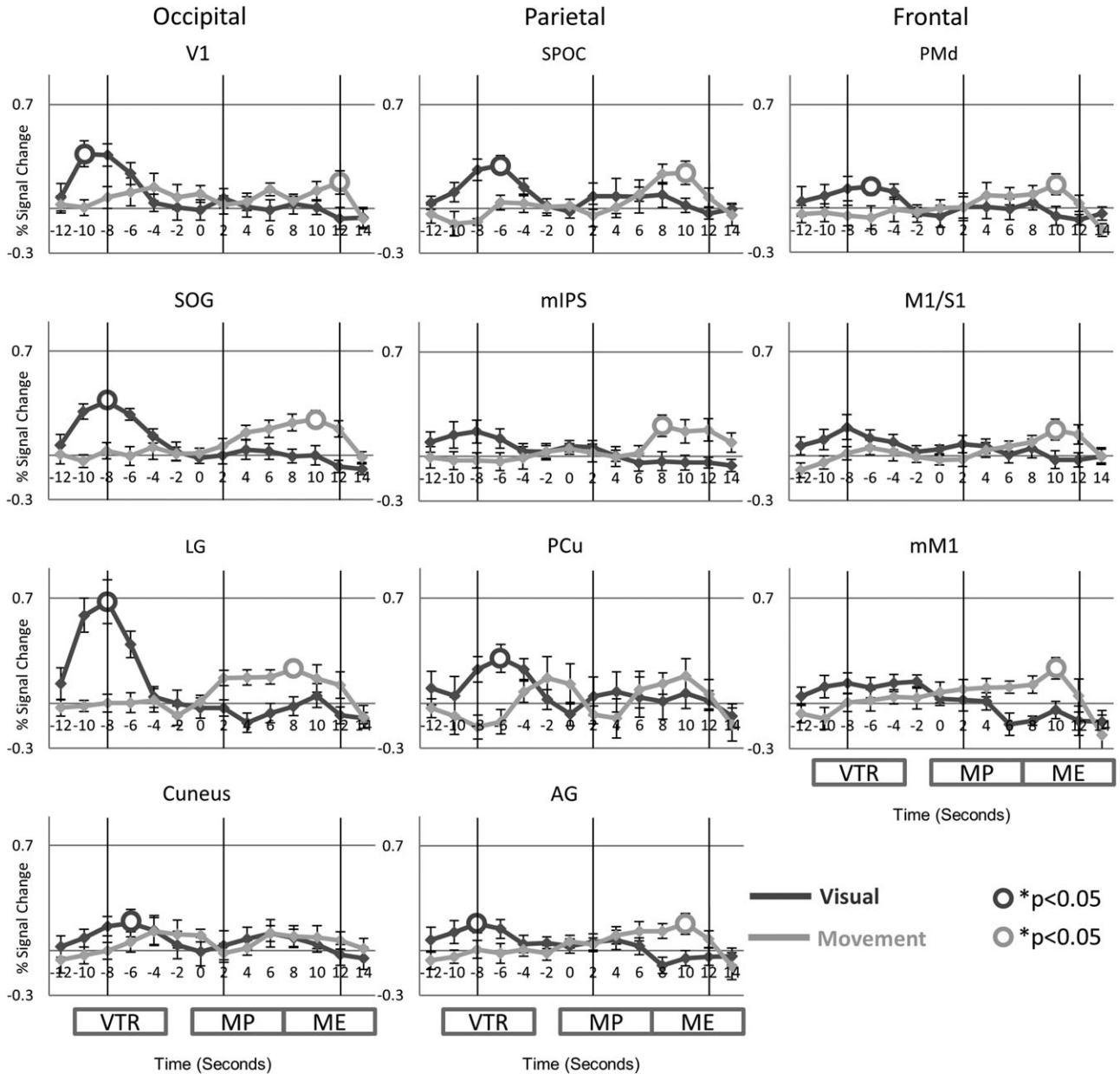

Figure 5. A plot of the time courses of visual and movement selectivity for left occipital (V1, SOG, cuneus, and LG), parietal (SPOC, mIPS, PCu, and AG), and frontal (PMd, M1/S1, and M1) left hemisphere brain regions. On the x-axis, time is in seconds and 0 indicates the start of the MP phase. The 3 black vertical lines indicate the times of peak activity noted in Figure 3 for the VTR, MP, and ME phases. The dark gray lines indicate the visually selective mean % signal change across subjects. This was calculated by subtracting the time courses for trials where the visual target was presented ipsilaterally (pro-reach left and anti-reach left) from trials where the visual target was presented contralaterally (pro-reach right and anti-reach right). The light gray lines indicate the movement direction selective mean % signal change across subjects. This was calculated by subtracting the time courses for trials with an ipsilateral motor goal (pro-reach left and anti-reach right) from trials with a contralateral motor goal (pro-reach right and anti-reach left). White open circles (○) indicate activity significantly greater than zero (one-sample *t*-test, $P < 0.05$). Error bars are SEM across subjects.

and the second a more prolonged movement peak that in most cases appears to arise late in the planning phase, dropping off just at execution. Second, although visual peaks are more predominant in the occipital areas as one would expect, the motor peak was widespread. In particular, occipital areas SOG and LG show a surprisingly robust "movement direction coding" during the planning phase (we will propose an alternative explanation for this in the discussion). In summary, it appears that movement direction selectivity engages the entire occipital–parietal–frontal reach network.

Although no areas in the right hemisphere met our localizer criteria, we performed a similar analysis on right SOG, mIPS, SPOC, and PMd by flipping the Talariach "x" coordinate and creating a 5 mm sphere ROI. These values were similar to right hemisphere coordinates for these areas reported by other papers (Vesia et al. 2010, Gallivan et al. 2011, Monaco et al. 2011; Chen et al. 2014). While right mIPS, SPOC, and PMd did not show much selectivity, right SOG showed a trend to prefer visual target direction early in the task, similar to left SOG. These right hemisphere data do not meet current statistical

standards for reporting fMRI data, but we have included these data as a Supplementary Fig. 8.

Transition of Visual-to-Movement Direction Coding through Time in the Anti-Reach Task

If one subtracts contrast #4 (visual direction tuning) from contrast #5 (motor direction tuning), this essentially reduces to a contrast between the left and right anti-reach conditions during MP [anti-reach left target – anti-reach right target]. Note that here, direction is defined in terms of stimulus location, so a negative value would indicate contralateral visual direction selectivity, whereas a positive value would indicate contralateral movement direction selectivity (in the anti-reach task). We henceforth refer to this integrated measure as our "visuo-movement" selectivity parameter. Figure 6 plots this parameter through time for 8 areas in the left hemisphere that have been selected to best represent the occipital–parietal–frontal reach network, ordered to correspond roughly to "early" (V1) through "late" (mM1) areas in the visuomotor transformation for reach. We performed paired *t*-tests between the visually and movement selective data at the time of peak visual (the minimum mean value) and peak movement (the maximum mean value) selectivity to indicate significantly higher visual or movement selectivity, respectively. We limited our comparisons to these 2 points in time to indicate the presence of significantly higher visual or movement direction selectivity in a brain area without needing to correct for multiple comparisons across all time points. As there were 2 *t*-tests, we performed a Bonferroni correction for 2 comparisons ($\alpha = 0.05 / 2$ comparisons $= 0.025$ corrected for $P < 0.05$).

As one might predict, only significantly higher visual selectivity was observed in V1, and only significantly higher movement selectivity was observed in mM1. SPOC and PCu also showed significantly higher visual selectivity, while AG also showed significantly higher movement selectivity. SOG and PMd showed both significantly higher visual and movement selectively. Also, as one would expect in the anti-reach task, the switch from visual coding to movement coding occurs around the time of the pro/anti instruction (although we could not establish this statistically because of the size of variance relative to the small visuomotor scores at this cross-over point). What is more remarkable, is the strong resemblance between these curves obtained from very different brain areas, ranging from some that have been categorized as strictly visual (V1) through various visuomotor areas to mM1. The next section further quantifies these observations.

Temporal Correlation of Direction Selectivity between Cortical Areas

To quantify some of the qualitative observations made above, we performed temporal correlations of visual, movement, and visuo-movement directional selectivity between the regions identified in Figure 4. To do this, we used the % BOLD signal change time series data from 12 s before the onset of MP (target presentation) to 12 s after (peak activity for motor execution as seen in Fig. 3). We then correlated between sites (r) by matching their BOLD signal changes for each scan in this time range. Note that the main contribution to these correlations likely came from the target coding phase and late planning phase for the visual and movement parameters respectively (Fig. 5), whereas the visuo-movement parameter was modulated throughout the entire sequence (Fig. 6).

Figure 7*A* shows the visual direction selectivity correlations between each brain area. The entries in this matrix have been ordered (top to bottom and left to right) based on the strength of correlation with V1, using the functional region from contrast 5. V1 was selected as the most obvious reference region for visual input to the system. The resulting correlation matrix shows a progressive drop in correlation down and to the left (as expected) progressing generally from more sensory regions like LG to more motor regions such as mM1. This can also be visualized as progression from darker red to lighter pink in the color scheme we have used for the matrix cells. These correlations were often significant (as indicated by bolded numbers) with a $P < 0.05$ with Bonferroni corrections for 10 comparisons [$\alpha = 0.05 / 10$ comparisons $= 0.005$ corrected for $P < 0.05$].

Figure 7*D* graphically represents the same data as Figure 7*A* as a network of correlations between our various ROI. The width of each line is scaled by the r^2 value for the 2 regions that it joins, with significant correlations highlighted in yellow ($P < 0.05$, non-significant correlations are shown in orange). This figure also helps to visualize "hub" areas in the visual domain, sprouting thick yellow lines (high correlations with yellow indicating significant correlations) toward numerous other areas, as opposed to thin orange lines (low correlations with orange indicating non-significant correlations). In the visual domain (Fig. 7*D*), one observes an extensive network of significant correlations including V1, SOG, mIPS, M1/S1, and PMd (i.e., these areas have many thick yellow lines), but largely excluding mM1 and PCu (i.e., these areas have mainly thin orange lines). Overall, SOG had the highest mean correlation (0.83) to all other areas in the visual domain.

Figure 7*B* similarly shows the movement direction selectivity correlations between each brain area. Here, mM1 was chosen as the most obvious reference motor region, such that the matrix entries are ordered based on the strength of correlation with mM1 (the functional region from contrast 5 was used). This resulted in a an ordering of sites nearly opposite to Figure 7*A*, except for a few regions (notably PCu) shifted to the right (meaning its correlations rank remained low) or left (e.g., SOG, meaning that it retained its relatively high rank in both representations). Again, this convention caused higher correlations to cluster in the upper-left of the matrix, many of these significant (bold) with a $P < 0.05$, Bonferroni corrected as in Figure 7*A*. For movement direction selectivity (arising mainly during the late planning phase; Fig. 7*E*) a network of significant correlations arose between the regions spanning SOG to mM1, including AG, SPOC, M1/S1, and PMd, but excluding the very thin "connections" to the early visual areas V1 and LG, as well as parietal areas aIPS, mIPS, and PCu. Perhaps surprisingly, SOG once again had the (marginally) highest overall mean correlation (0.75) to all other regions in the movement domain. AG also had a mean correlation of 0.75, and these regions appear (along with SPOC) as prominent "hubs" in Figure 7*E*.

Figure 7*C* provides a similar plot, but in this case using the visuo-movement parameter from Figure 6. In this case there is no obvious reference region or order, so we ordered the chart from highest to lowest mean correlation across all sites (lower row in dark gray), such that SOG ended up in the upper-left cell with (once again) the highest mean correlation to other areas (0.86). Although these plotting conventions tended to place higher correlations to the upper-left of the matrix, the overall distribution of high and significant correlations was broader in this domain (Fig. 7*C*), extending further down and to the right than the individual visual and movement domains (Fig. 7*A*,*B*). In addition to SOG, mIPS, AG, and SPOC showed mean correlations

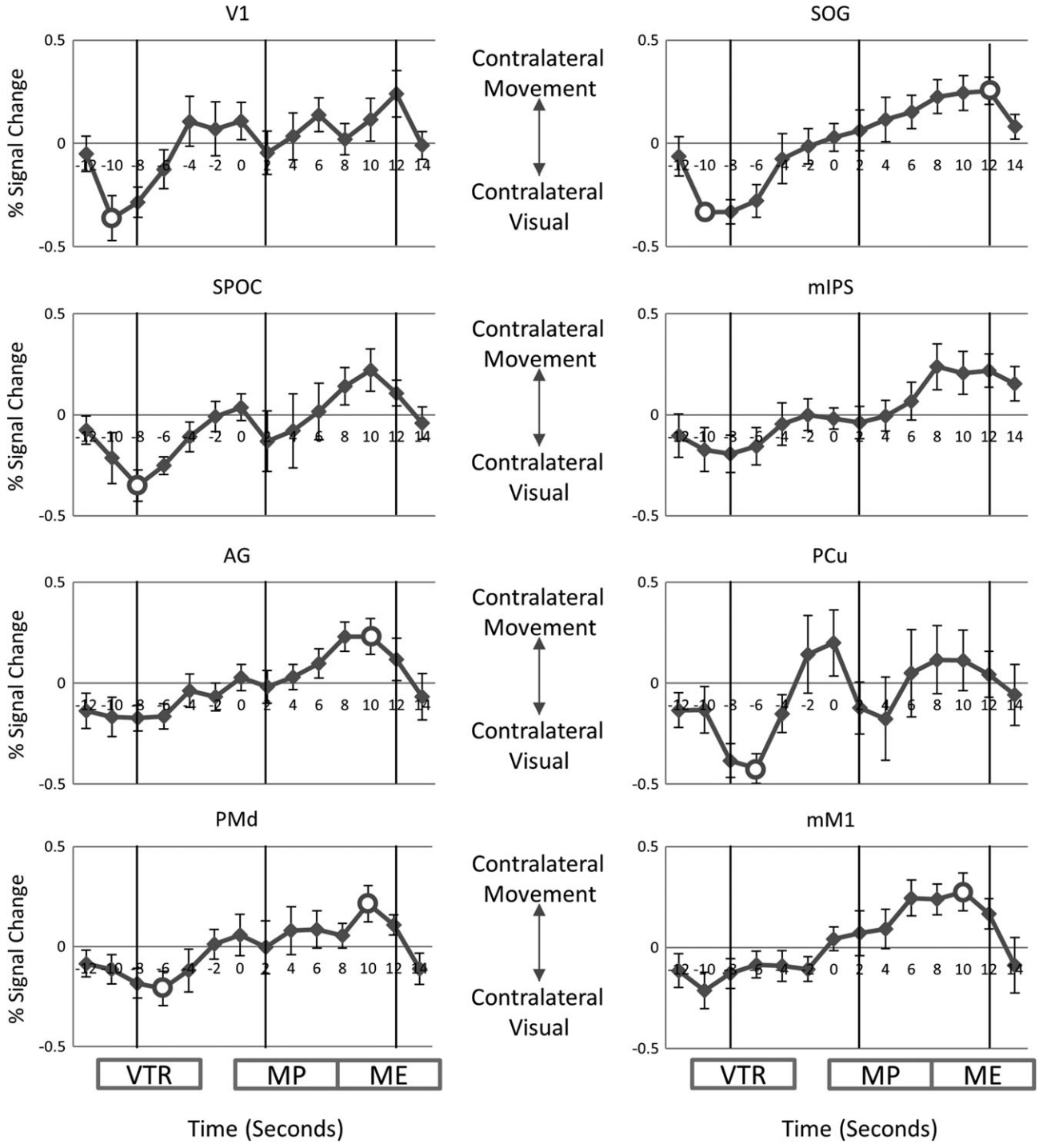

Figure 6. Visuo-movement direction selectivity plotted through time for left V1, SOG, SPOC, mIPS, AG, aIPS, PMd, and M1. This was calculated by subtracting the visual selective time course data from the movement direction selective time course data displayed in Figure 5. Thus, a negative % signal change indicates visual selectivity and a positive score indicates movement direction selectivity. On the *x*-axis, time is in seconds and 0 indicates the start of the MP phase. The 3 black vertical lines indicate the times of peak activity noted in Figure 3 for the VTR, MP, and ME phases, and gray vertical lines indicate their onset. Open circles (○) indicate significantly greater coding for that coordinate system as revealed by a paired *t*-test ($P < 0.05$). Error bars are SEM across subjects.

above 8.0, with SPOC being noteworthy for being the only site that was significantly correlated to all other areas ($P < 0.05$ with Bonferroni corrected as in Fig. 7A). These 4 areas emerge as major correlation "hubs" in Fig. 7F, as nearly all of the correlations are robust and significant (with PCu remaining the main exception). These analyses suggest that, despite overall biases toward visual or movement function between different sites, the entire occipital–parietal–frontal reach network is involved in the visuomotor transformation for a memory-guided reach task.

When these values were calculated between all possible pairings of our identified ROI, we obtained overall *r* values of 0.739 ± 0.13 for visual, 0.652 ± 0.20 for movement, and 0.799 ±

A Visual Correlations (r)

											Scale
V1	1										
LG	**0.97**	1									1.00
SOG	**0.95**	**0.94**	1								0.70
mIPS	**0.86**	**0.83**	**0.82**	1							0.40
M1S1	**0.84**	**0.77**	**0.87**	**0.87**	1						0.10
aIPS	**0.78**	0.71	**0.75**	**0.90**	**0.87**	1					
PMd	**0.77**	**0.73**	**0.87**	0.69	**0.88**	**0.74**	1				
AG	**0.77**	0.72	**0.83**	**0.87**	**0.81**	**0.79**	0.66	1			
SPOC	**0.74**	0.70	**0.85**	0.59	**0.82**	0.55	**0.92**	0.67	1		
mM1	0.59	0.58	0.67	**0.79**	0.70	0.66	0.57	**0.75**	0.47	1	
PCu	0.54	0.55	0.72	0.47	0.65	0.42	**0.84**	0.59	**0.87**	0.52	1
	V1	LG	SOG	mIPS	M1S1	aIPS	PMd	AG	SPOC	mM1	PCu

B Movement Correlations (r)

											Scale
mM1	1										
AG	**0.91**	1									1.00
PMd	**0.85**	**0.94**	1								0.70
SOG	**0.82**	**0.92**	**0.92**	1							0.40
SPOC	**0.79**	**0.79**	**0.79**	**0.82**	1						0.10
LG	**0.73**	**0.82**	**0.85**	**0.87**	0.62	1					
M1S1	**0.73**	0.69	**0.78**	**0.82**	**0.79**	0.60	1				
aIPS	0.68	0.64	0.72	**0.74**	**0.78**	0.44	**0.96**	1			
mIPS	0.62	0.69	0.70	**0.78**	**0.81**	0.59	0.71	0.71	1		
PCu	0.53	0.53	0.49	0.46	0.70	0.17	0.39	0.50	0.65	1	
V1	0.39	0.21	0.37	0.38	0.45	0.10	0.66	0.67	0.33	0.44	1
	mM1	AG	PMd	SOG	SPOC	LG	M1S1	aIPS	mIPS	PCu	V1

C Visuo-Movement Correlations (r)

											Scale
SOG	1										
mIPS	**0.93**	1									1.00
AG	**0.92**	**0.96**	1								0.70
SPOC	**0.90**	**0.93**	**0.90**	1							0.40
PMd	**0.91**	**0.85**	**0.88**	**0.90**	1						0.10
mM1	**0.89**	**0.87**	**0.94**	**0.79**	**0.84**	1					
M1S1	**0.81**	**0.90**	**0.86**	**0.83**	**0.81**	**0.83**	1				
LG	**0.93**	**0.77**	**0.80**	**0.76**	**0.79**	**0.81**	0.64	1			
PCu	0.72	0.72	0.70	**0.87**	**0.80**	0.55	**0.83**	**0.81**	1		
V1	**0.84**	**0.75**	0.71	**0.78**	0.72	0.68	**0.73**	**0.84**	0.65	1	
aIPS	0.72	**0.85**	**0.83**	**0.76**	0.72	**0.78**	**0.95**	0.54	0.54	0.69	1
Mean	0.86	0.85	0.83	0.81	0.78	0.73	0.79	0.73	0.59	0.69	0.55
	SOG	mIPS	AG	SPOC	PMd	mM1	M1S1	LG	PCu	V1	aIPS

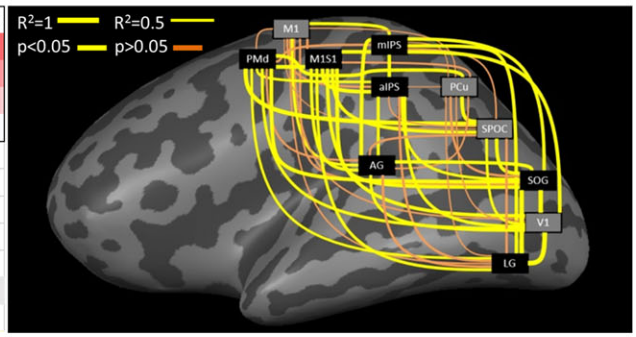

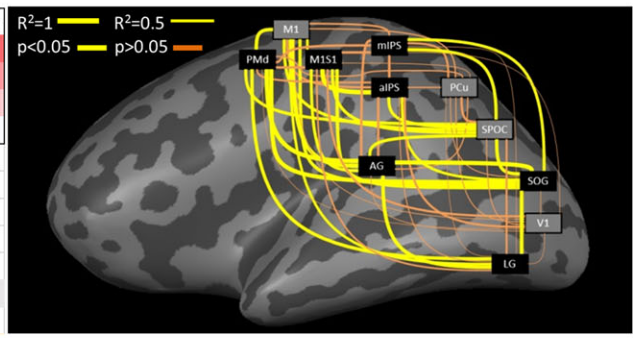

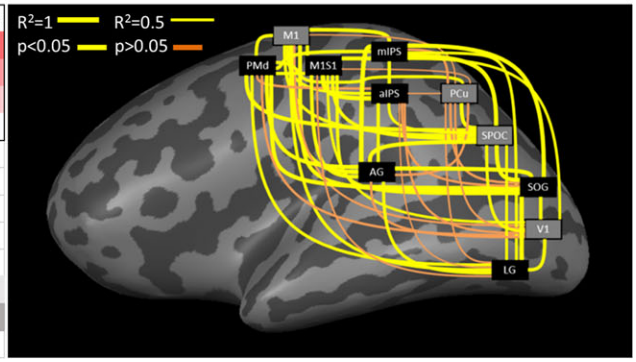

Figure 7. Correlations through time between regions derived from visual, movement, and visuo-movement spatial parameters. (*A–C*) Matrices showing correlations (*r*) through time between all areas for each spatial domain tested (redundant entries in upper-right half are omitted). A continuous color scale is used to indicate the strength of correlation (*r*), i.e., with white close to 0.1 and red close to 1.0, and significant correlations ($P < 0.05$, Bonferroni corrected) are bolded. Site correlations were derived by comparing data points from each point in time derived for the 10 movement-selective areas in the left hemisphere correlated for visual selectivity from target presentation (−12 s) to peak motor execution activation (+12 s), time-locked to the onset of MP. (*A*) Visual Correlations. The order of areas is based on strength of correlation with V1. (*B*) Movement Correlations. The order of areas is based on strength of correlation with mM1 (the motor output from the system). (*C*) The time courses for the 10 motor-selective areas correlated for visuo-movement selectivity. The order of areas is based on strength of the mean correlation with the other areas (shown in lower row). (*D–F*) Graphical representations of the strength of correlation between left hemisphere brain areas for visual (*D*), movement (*E*), and visuo-movement (*F*) correlations corresponding to data from A, B, and C, respectively. The thickness of the line indicates the r^2 value, with a thin line being close to 0 and a thick line close to 1. For these plots we used r^2 to increase the difference between highly correlated and less correlated areas. These data are superimposed on a left hemisphere "inflated brain" from a typical subject where light gray signifies gyri and dark gray signifies sulci. See Table 4 for site abbreviations. Brain areas in black boxes are superficial and those in gray boxes appear on the medial side of the inflated brain.

0.10 for visuo-movement (mean ± SD) selectivity indices. To test if they were significantly higher than zero, we performed 3 one-sample *t*-tests on the mean *r* scores for each brain area, comparing zero to visual ($t(10) = 37.129$, $P < 0.001$), motor ($t(10) = 18.771$, $P < 0.001$), and visuomotor ($t(10) = 45.755$, $P < 0.001$) selectivity frames, all of which were significant. To test for differences between selectivity frames and to investigate differences between brain regions, we performed an ANOVA on the *r* values with selectivity frame (visual, movement, and visuo-movement) and the 11 brain areas as fixed factors. The ANOVA was significant ($F(32,1) = 5.689$, $P < 0.001$) and showed significant main effects for selectivity frame ($P < 0.001$) and brain area ($P < 0.001$), as well as a significant interaction between selectivity frame and brain area ($P < 0.005$). Bonferroni post hoc tests on selectivity frames revealed that visual, movement, and visuo-movement selectivity were all significantly different from each other. Bonferroni post hoc tests on brain areas revealed that the PCu and V1 showed significantly lower

correlations than several other brain areas (for PCu: AG, aIPS, mM1, mIPS, PMd, M1/S1, SOG, and SPOC; for V1: AG, mIPS, PMd, M1/S1, SOG, and SPOC). Thus, both retrospective target direction and prospective reach direction were important for describing correlations between these networks at different phases, and a visuo-movement parameter that captured both of these provided the best overall description.

Discussion

In this study, we used an event-related fMRI design to investigate several key questions. To summarize, the first was to differentiate which cortical areas are involved in spatial target representation, reach MP, and reach ME. This analysis revealed selective, bilateral PMd and right pIPS activation during the target representation phase, whereas an entire occipital–parietal–frontal reaching network was activated during the motor planning and execution phases. The second question we aimed to answer was, during motor planning, which brain areas are directionally selective in visual or motor coordinates? During our planning phase, the left cuneus showed significant contralateral visual selectivity, but the majority of directionally selective occipital, parietal, and frontal activation was tuned for contralateral reach direction. Observing the time courses of these directional parameters across all 3 phases of our task, we observed that most areas showed visual selectivity following target presentation and most areas showed movement selectivity late in the planning phase, but all reach-related areas showed a progressive visuomotor transition when these measures were collapsed into a single visuo-movement parameter. Likewise, when we correlated these parameters through time between different areas, we found overlapping but distinct visual and motor networks, but that all of the areas activated in occipital, parietal, and frontal cortex were correlated in terms of the visuo-movement index. In the following sections, we will discuss each of these findings in more detail.

General Activation During Visual Target Memory, Reach Planning, and Reach Execution

Many previous fMRI studies have implicated superior occipital–parietal–frontal cortex in visually guided reaching (Astafiev et al. 2003, Connolly et al. 2003; Medendorp et al. 2003, 2005; Prado et al. 2005; Fernandez-Ruiz et al. 2007; Beurze et al. 2009; Cavina-Pratesi et al. 2010; Fabbri et al. 2012; Konen et al. 2013; Chen et al. 2014). However, to our knowledge none of these clearly separated the 3 phases of target representation, MP, and ME through time. To do this within the spatiotemporal limitations of fMRI, we required a paradigm with a series of instructions and delays which likely introduced more cognitive aspects to the task one would see during online control, but with this caveat in mind, we were able to trace both general and direction-specific activation through those 3 phases. Most of our ROI showed different degrees of time-locked activation during target representation, planning, and execution (Fig. 3), depending on whether the region was more visual (e.g., SOG) or motor (e.g., PMd), but here we will restrict our discussion to significant clusters of activation during these 3 phases (Fig. 2).

Our analysis of the target representation phase (Fig. 2A) revealed limited activation in bilateral PMd and right pIPS, perhaps related to spatial working memory (Courtney et al. 1996; Srimal and Curtis 2008) or activity related to preparatory set (Culham et al. 2006, Chen et al. 2014). Chen et al. (2014) found a broader range of occipital–parietal–frontal activation during the target memory phase of their paradigm. Our target memory phase was followed by target planning and then execution, whereas their target memory phase was followed immediately by motor execution. This may have precipitated earlier preparatory activity in their paradigm and thus explain the difference. Activation in the parietal cortex is consistent with the uncertainty condition found in Gertz and Fiehler (2015), though their parietal activation was in the left hemisphere and ours was in the right. This difference could be due to the additional delay we added before the pro/anti instruction or the way we defined ROI (we derived coordinates from peak voxels in our own data whereas they used published coordinates).

Note that in our paradigm, subjects could not anticipate the required movement plan or derive it from the visual stimulus until the pro/anti instruction was given at the start of the second delay. During this MP phase (Fig. 2B), we observed widespread activation in the classic parieto–frontal reach network, including SPOC, mIPS, SMA, PMd, and M1 (Culham et al. 2006; Gallivan and Culham 2015). Comparing this widespread planning activation to the limited activation that was observed in the target representation phase suggests that previous studies that combined these 2 phases (Medendorp et al. 2003, Fernandez-Ruiz et al. 2007) were mainly reporting activity related to visuomotor transformations and/or MP, as opposed to target memory. We also observed considerable activation of occipital cortex, including LG, IOG, and SOG, during the second delay, a phenomenon known as "occipital reactivation" (Singhal et al. 2013), which we will discuss further in subsequent sections. In all these lobes, lateral cortex activation was greater in the left hemisphere contralateral to the hand, consistent with previous studies (Connolly et al. 2003; Fernandez-Ruiz et al. 2007; Bernier et al. 2012; Gertz and Fiehler 2015). Finally, all of these regions of activation became even more extensive (relative to controls) in the ME phase (Fig. 2C), also extending into prefrontal (e.g., IFG) and inferior parietal (e.g., SMG) areas that might be associated with cognitive aspects of the task, such as guidance of the movement based on spatial memory (Gallivan and Culham 2015). In general, through our 3 phases we observed a general spread and ramping up of activation relative to controls throughout occipital–parietal–frontal cortex, presumably as different constraints were added to the task (target memory, rule-based visuomotor transformation, MP, and actual execution) while retaining past information.

Directional Selectivity During MP

A second goal of our study was to look at cortical direction selectivity during MP, and determine which areas are selective for visual target direction and movement direction. Note that our paradigm was not designed to explicitly separate cognitive events such as attention vs. intention (Colby and Goldberg 1999; Andersen and Buneo 2002), but can only disambiguate directional selectivity relative to our objective measures (visual target direction and movement direction). Clearly attention must play a role in our task: subjects likely attended to remembered target direction in the first memory delay (Rizzolatti et al. 1987), and motor goal direction in the second planning delay, switching attention to the opposite hemifield during the "anti" trials (Rolfs et al. 2013). The latter must especially play a role in the switching of directional tuning from stimulus to motor goal that we observed in occipital cortex (see below for details). On the other hand, massive recruitment of the parieto–frontal reach network that we observed in the late planning and early execution phase of our task (much of which proved to be

movement direction selective) is most likely related to the intention to move (Andersen and Buneo 2002; Cisek and Kalaska 2010).

In the following, more detailed discussion, we will only consider regions that showed significant clusters of activation. One of the main aims of our visual and movement direction selective contrasts was to localize established reach-related regions for a more detailed temporal analysis on their time course data. We further restricted this analysis to the second delay (MP) because 1) this gave much more activation in general than the first delay, 2) the first delay could only yield visual directional selectivity, 3) selective combinations of our pro- and anti-reach data could isolate visual vs. motor selectivity during the second delay, and (4) the ME phase was biased by somatomotor activation related to the arm movement itself.

Contralateral Direction Tuning and Handedness

Although we found scattered, non-specific clusters of activation of ipsilateral tuning (for either target or movement, primarily in the right hemisphere) in general, we found a fairly widespread tendency toward contralateral direction tuning within the occipital–parietal–frontal reach system in the left hemisphere. This does not necessarily mean that these areas only code one direction of target or movement (indeed most areas showed responses for both directions; Supplementary Figs. 5–7). Instead, it means that there was more activation for contralateral than ipsilateral movement. This generally agrees with previous investigations of occipital, parietal, and prefrontal activity based on fMRI (Medendorp et al. 2003, 2005; Filimon et al. 2009; Vesia and Crawford 2012; Gertz and Fiehler 2015), MEG (Van Der Werf et al. 2010), TMS (Vesia et al. 2010), patients (Khan et al. 2007), and primate neurophysiology (Gail and Andersen 2006; Gail et al. 2009; Westendorff et al. 2010). Contralateral movement tuning is more surprising in S1 and M1 (because they are associated with moving the contralateral hand in both directions), but this is easily explained. In our setup, the right hand started from the left side, so it moved more for rightward targets, thus predicting more activation for contralateral targets.

Further, this contralateral tuning was always in the left hemisphere, contralateral to the right hand used in the study. This is consistent with several previous fMRI studies (Connolly et al. 2003; Fernandez-Ruiz et al. 2007; Bernier et al. 2012; Gertz and Fiehler 2015). This asymmetry could also relate to the statics of fMRI, i.e., the way that several neural signals might need to combine to produce significant effects at the level of the BOLD signal. Here, this likely involves interactions between hand lateralization and visual hemifield lateralization (Perenin and Vighetto 1988; Rossetti et al. 2003, Medendorp et al. 2005; Beurze et al. 2007; Blangero et al. 2008, Gallivan et al. 2011; Vesia and Crawford 2012). In particular, greater activation is expected in the cortex contralateral to the hand (Snyder 2000; Medendorp et al. 2005), and as mentioned above, this effect would be magnified in motor areas in our experiment because the right hand moves more to the right than it does for left targets. In more visual areas, there may also an influence of handedness on attention (Perry et al. 2015).

Visual Directional Selectivity

The visual directionally selective contrast in our task found that only the left cuneus showed significant activation for visually contralateral targets regardless of the motor requirement. This implies that there is a region in occipital cortex that is specifically concerned with retaining the visual direction of the original stimulus, regardless of whether subjects are planning a movement in that direction or in the opposite direction. Makino et al. (2004) previously found that the cuneus can be activated by both visual search and memory search, and suggest that it may be responsible for attentional shifts in short- and long-term memory. These search and attentional functions may be aided by a visual representation of an object in space, regardless of and independent from the motor requirement of a task. Nonetheless, the extent of visual lateralized activation that we observed here, restricted to cuneus, was rather modest compared with the visually-tuned BOLD response observed throughout occipital and parietal cortex during reversing prism adaptation (Fernandez-Ruiz et al. 2007). We will return to this apparent contradiction in a later subsection.

Movement Direction Selectivity

During MP, we observed relatively widespread movement-tuned direction selectivity in the left parieto–frontal cortex, including mIPS, SPOC, AG, aIPS, PMd, and M1/S1. This generally agrees with previous reach (and saccade) investigations that have used the pro/anti task combined with fMRI (Medendorp et al. 2005), MEG (Van Der Werf et al. 2008, 2010), and primate neurophysiology (Gail and Andersen 2006; Gail et al. 2009; Westendorff et al. 2010). Consistent with this, PMd neurons are active during the delay period preceding an instructed movement, as well as tuned for the direction and distance of reaches with either hand (Weinrich and Wise 1982; Caminiti et al. 1991; Messier and Kalaska 2000; Cisek et al. 2003). It is perhaps more surprising that we found several occipital areas linked to movement direction during the planning phase, including SOG. Likewise, Chen et al. (2014) found directionally selective occipital activation during their ME phase. One does not generally associate occipital cortex with MP, but note that in the pro/anti paradigm, subjects may use a strategy of imagining a target that is either contiguous with, or opposite to the original visual stimulus. These findings suggest that occipital cortex plays a more important role in action planning than is often assumed (Pasternak and Greenlee 2005; Gutteling et al. 2015).

Reconciling Studies of Spatial Tuning for Reach Planning

The Fernandez-Ruiz et al. (2007) prism reversal study showed visual tuning in most of the same occipital–parietal regions that showed movement tuning in the pro-/anti-reach task (see also Gertz and Fiehler 2015). This appears to be a contradiction, but Ferandez-Ruiz et al. (2007) offered an explanation based on discriminating the parameter being represented (i.e., visual target, vs. movement goal, vs. movement direction) and the coordinate frame used to represent this (i.e., retinal coordinates vs. body-fixed coordinates). According to this notion, areas such as mIPS do not encode visual target direction (that contradicts the current study) or movement direction (which contradicts the prism-reversal study). Instead, they may encode the direction of the imagined goal in retinal coordinates (which would be linked to retinal input during prism reversal, but reversed relative to retinal input in the anti-reach task). This model fits most of our occipital–parietal regions, with exception of cuneus (which appears to encode visual stimulus direction in both tasks; see above) and AG, which appears to encode extrinsic movement direction in both tasks, perhaps in somatosensory coordinates (Vesia et al. 2006, 2010; Fernandez-Ruiz et al. 2007; Vesia and Crawford 2012).

A complication to this scheme is that Kuang et al. (2016) recorded action potentials from intraparietal cortex in monkeys trained on both the prism reversal task and the pro-/anti-reach task, and found that some neurons did encode the goal in visual coordinates, but most encoded movement direction. They reconciled this finding with fMRI results by noting that local field potentials—which may drive the BOLD response—agreed better with the visual goal prediction. Alternatively, the massive amount of training required for monkeys to do such tasks may have altered synaptic organization, whereas the human subjects received minimal training. However, these are matters of degree, not fundamental differences. Either way, it appears that the occipital–parietal–frontal reach planning system can simultaneously encode 3 spatial variables: visual stimulus direction, the goal in visual coordinates, and extrinsic movement direction.

Visual, Movement, and Visuo-movement Selectivity Through the Entire Task

Some of the most interesting findings in this experiment derived from plotting the time courses of visual and movement selectivity (Fig. 5) for all of our ROI. A number of neurophysiological studies have followed the time course of directional tuning during a pro/anti task (e.g., Zhang and Barash 2000; Gail and Andersen 2006; Gail et al. 2009). However, to our knowledge, we are the first to extract these variables from pro-/anti-reach data in the human brain and examine their time course through separate target representation, planning, and reach execution phases. Although fMRI suffers by comparison in spatiotemporal resolution, it compensates by allowing one to compare these responses across the entire brain. In short, although some areas showed primarily visual direction tuning following presentation of the target and some primarily showed movement direction tuning late in the planning phase, most of our ROI showed both of these responses. We shall consider these "lobe-by-lobe," and then consider the network.

Occipital Cortex

Not surprisingly V1 and cuneus primarily showed visually selective activation, as numerous previous studies have shown human V1 to code visual stimulus responses (Engel et al. 1997; Singh et al. 2000), and perhaps even visual memory responses (Pratte and Tong 2014; Malik et al. 2015). As mentioned above, the finding that only left occipital areas showed direction selectivity was surprising, and might relate to attentional enhancement related feedback from the contralateral hand and working in that hands preferred areas of space (Gallivan et al. 2011; Perry et al. 2015). Further, SOG and LG showed both visual and "motor" selectivity. It is possible that these structures initially responded to the visual stimulus, but after the pro/anti instruction were involved in imagining a virtual target that could be flipped opposite to the actual stimulus in the case of anti-reach trials (Rolfs et al. 2013). This could explain the phenomenon of occipital reactivation during reaches, and could involve re-entrant feedback from motor systems (Singhal et al. 2013).

Parietal Cortex

To different degrees, all of our parietal structures showed dual spatial selectivity, but SPOC and AG stood out as "hub" areas that showed both visual and movement selective activation. Consistent with our results, recent studies have implicated SPOC as a visually-guided reaching area (Culham et al. 2006; Filimon et al. 2009; Vesia et al. 2010; Gallivan and Culham 2015). Previous studies on AG, however, have implicated it as coding the motor output of a task (Fernandez-Ruiz et al. 2007; Vesia et al. 2010), making the visually selective activation unexpected. However, this might indicate transformation of visual signals into somatosensory signals, as suggested by its general role in left–right space discrimination (Hirnstein et al. 2011). The PCu was found to be visually selective during the target representation phase. This activation could be related to visuospatial imagery (Cavanna and Trimble 2006), although it did not show the anti-reach reversal we observed for SOG. It is also unclear why both PCu and SPOC show slight reversals from motor to visual planning around the time motor planning begins. These reversals did not reach significance, but if they represent a real result, we speculate this may be due to a visual re-activation once the movement is known.

mIPS only showed directionally selective motor activation. This is consistent with the suggestion in Fernandez-Ruiz et al. (2007), discussed above, that such areas would show movement tuning in an anti-reach task. However, the lack of an early visual response is surprising given that it has been linked to both reach and saccade planning, attention, and visual working memory (Curtis et al. 2004; Curtis and Connolly 2008; Srimal and Curtis 2008; Jerde et al. 2012). Medendorp et al. (2005) found that for saccades, retinotopic IPS (similar to mIPS) coded the visual location of a target before the pro/anti instruction and the motor direction afterwards. It is important to note, however, that these areas were selected by different methods (an independent localizer vs. peak voxel ROI) and that activation for saccades may differ from the reach planning network.

Frontal Cortex

Left PMd showed visually selective activation during target representation and motor selectivity during ME. Previous research has found left PMd activation for right arm reaching (Medendorp et al. 2005; Bernier et al. 2012; Gertz and Fiehler 2015) and implicated the region in transforming visuospatial information into motor codes (Medendorp et al. 2005; Beurze et al. 2007), which supports our motor-selective finding. There is also evidence from multivariate fMRI techniques for target selective coding in PMd (Gallivan et al. 2011; Fabbri et al. 2012), which may help explain the visually-selective encoding we noted during the target representation phase. Finally, a recent neurophysiological study suggests that frontal eye fields progressively transition from a target to movement code, even when planning pro-saccades (Sajad et al. 2016).

Visuomotor Selectivity in all Areas

One of our more striking findings was that when we described our occipital–parietal–frontal regions with the use of a visuomovement parameter (derived from the anti-reach data) and plotted these data through the entire time course of our task (Fig. 6), every single area, from V1 to M1, looked remarkably similar (with the exception of a mid-task "bump" in some areas like PCu, around the time of the pro/anti instruction). This appears to illustrate a very simple but profound message: despite the many functional differences between these areas (like those described above and by many other authors), an entire occipital–parietal–frontal network is engaged in the transformation of visual stimuli into motor acts; Not only at different serial stages of processing, but also through the entire duration of

the task (for example, see the occipital reactivation in our SOG data). In this sense, even though visuomotor transformations can be observed within single structures and even single neurons (e.g., Sadeh et al. 2015; Sajad et al. 2015, 2016), almost the entire cortex is engaged in the entirety of such transformations. This is further supported at the motor output level by recent evidence of upper limb muscles initially encoding the location of the visual stimulus rather than the movement goal for anti-reaching in humans (Gu et al. 2016).

Spatiotemporal Correlations for Visual, Movement, and Visuo-Movement Selectivity

We were able to quantitatively summarize our measures of early visual tuning and late movement tuning, and organize these into spatiotemporally correlated modules by correlating these measures through time between left hemisphere ROI (Fig. 7A–C), and using these correlations to construct a network of spatiotemporally correlated modules (Fig. 7D–F). This resulted in 2 widely distributed, overlapping networks: the first strongly correlated to visual input from V1 (Fig. 7A,D), and the second strongly correlated with motor output from M1 (Fig. 7B, E). However, it was the visuo-movement parameter that yielded the best overall correlations between areas (Fig. 7C,F). The full set of sensory, motor, and sensorimotor correlations for all areas are illustrated graphically in Figures 7D–F. Although correlation does not imply causation (for example, some of these correlations may have been due to common inputs, including attentional processes), the structure of these networks appear to agree well with the known anatomy of the dorsal visual stream system and reach systems (Vesia and Crawford 2012; Gallivan and Culham 2015). Further, it suggests that almost the entire network is concerned with transforming retrospective visual direction into prospective movement direction (Curtis 2006).

Of these areas, SOG stood out as having the highest mean correlations against all other areas in all 3 domains: visual, movement, and visuo-movement. This is perhaps surprising for an occipital area, and might be related to a key role for SOG in encoding the potential or actual egocentric goal, independent of initial stimulus (Gallivan et al. 2011; Chen et al. 2014), or occipital cortex receiving visuospatial attention or motor signals from parietal cortex (Lauritzen et al. 2009; Singhal et al. 2013; Perry et al. 2015). SPOC and mIPS also showed high correlations in the visuo-movement domain, with SPOC being noteworthy as the only shared region that significantly correlated with all other areas in the visuo-movement. This seems consistent with SPOC having a prominent role in representation of target location for reach (Vesia et al. 2010; Vesia and Crawford 2012). However, several other areas (LG, SOG, M1/S1, PMd, and AG) significantly correlated to both V1 in the visual domain and mM1 in the motor domain, so this transformational role is not unique to one area. Nor was it trivially required, because PCu showed relatively weakest correlations in all of the spatial domains that we tested. This may be task specific, because PCu has been implicated in other allocentric functions (Uchimura et al. 2015).

Although dorsal parietal cortex often gets the most attention in the sensorimotor literature, AG—an inferior parietal area—also showed significant visual correlation with V1, movement correlation with mM1, and visuo-movement correlations with most areas (except V1 and PCu), although its overall visual correlations were less than its movement correlations. Together with its multiple roles in coding motion in external space (Fernandez-Ruiz et al. 2007; Vesia and Crawford 2012), discrimination of left space from right (Hirnstein et al. 2011), controlling multiple effectors (Vesia et al. 2010), and in agency (Farrer et al. 2008), this might suggest that AG plays a central role in monitoring the awareness of ones actions within external space. In comparison, our current data suggest that other sensory areas like cuneus and SOG may be more concerned with monitoring events and goals in visual space. This again is consistent with the notion that the brain simultaneously monitors space in multiple frames. Overall, these data suggest that the brain uses a broadly distributed, common visuomotor code for memory guided reach, and thus the need for so many network nodes likely arises from other cognitive demands.

Supplementary Material

Supplementary material can be found at: http://www.cercor.oxfordjournals.org/.

Notes

Conflict of Interest: None declared.

References

Andersen RA, Buneo CA. 2002. Intentional maps in posterior parietal cortex. Annu Rev Neurosci. 25:189–220.

Astafiev SV, Shulman GL, Stanley CM, Snyder AZ, Van Essen DC, Corbetta M. 2003. Functional organization of human intraparietal and frontal cortex for attending, looking, and pointing. J Neurosci. 23:4689–4699.

Berman R, Colby C. 2009. Attention and active vision. Vision Res. 49:1233–1248.

Bernier P-M, Cieslak M, Grafton ST. 2012. Effector selection precedes reach planning in the dorsal parietofrontal cortex. J Neurophysiol. 108:57–68.

Bernier P-M, Grafton ST. 2010. Human posterior parietal cortex flexibly determines reference frames for reaching based on sensory context. Neuron. 68:776–788.

Beurze SM, de Lange FP, Toni I, Medendorp WP. 2007. Integration of target and effector information in the human brain during reach planning. J Neurophysiol. 97:188–199.

Beurze SM, de Lange FP, Toni I, Medendorp WP. 2009. Spatial and effector processing in the human parietofrontal network for reaches and saccades. J Neurophysiol. 101: 3053–3062.

Beurze SM, Toni I, Pisella L, Medendorp WP. 2010. Reference frames for reach planning in human parietofrontal cortex. J Neurophysiol. 104:1736–1745.

Blangero A, Gaveau V, Luauté J, Rode G, Salemme R, Guinard M, Boisson D, Rossetti Y, Pisella L. 2008. A hand and a field effect in on-line motor control in unilateral optic ataxia. Cortex. 44 (5):560–568.

Caminiti R, Johnson PB, Galli C, Ferraina S, Burnod Y. 1991. Making arm movements within different parts of space: the premotor and motor cortical representation of a coordinate system for reaching to visual targets. J Neurosci. 11 (5): 1182–1197.

Cavanna AE, Trimble MR. 2006. The precuneus: a review of its functional anatomy and behavioural correlates. Brain. 129: 564–583.

Cavina-Pratesi C, Monaco S, Fattori P, Galletti C, McAdam TD, Quinlan DJ, Goodale MA, Culham JC. 2010. Functional magnetic resonance imaging reveals the neural substrates of

arm transport and grip formation in reach-to-grasp actions in humans. J Neurosci. 30:10306–10323.
Chen Y, Monaco S, Byrne P, Yan X, Henriques DYP, Crawford JD. 2014. Allocentric versus egocentric representation of remembered reach targets in human cortex. J Neurosci. 34: 12515–12526.
Cisek P, Kalaska JF. 2010. Neural mechanisms for interacting with a world full of action choices. Annu Rev Neurosci. 33: 269–298.
Cisek P, Crammond DJ, Kalaska JF. 2003. Neural activity in primary motor and dorsal premotor cortex in reaching tasks with the contralateral vs. ipsilateral arm. J Neurophysiol. 89: 922–942.
Colby CL, Goldberg ME. 1999. Space and attention in parietal cortex. Annu Rev Neurosci. 22:319–349.
Connolly JD, Andersen RA, Goodale MA. 2003. FMRI evidence for a "parietal reach region" in the human brain. Exp Brain Res. 153:140–145.
Connolly JD, Goodale MA, Cant JS, Munoz DP. 2007. Effector-specific fields for motor preparation in the human frontal cortex. Neuroimage. 34:1209–1219.
Connolly JD, Goodale MA, DeSouza JF, Menon RS, Vilis T. 2000. A comparison of frontoparietal fMRI activation during anti-saccades and anti-pointing. J Neurophysiol. 84:1645–1655.
Courtney SM, Ungerleider LG, Keil K, Haxby JV. 1996. Object and spatial visual working memory activate separate neural systems in human cortex. Cereb Cortex. 6:39–49.
Culham JC, Cavina-Pratesi C, Singhal A. 2006. The role of parietal cortex in visuomotor control: what have we learned from neuroimaging? Neuropsychologia. 44:2668–2684.
Curtis CE, Connolly JD. 2008. Saccade preparation signals in the human frontal and parietal cortices. J Neurophysiol. 99 (1): 133–145.
Curtis CE, Rao VY, D'Esposito M. 2004. Maintenance of spatial and motor codes during oculomotor delayed response tasks. J Neurosci. 24 (16):3944–3952.
Curtis CE. 2006. Prefrontal and parietal contributions to spatial working memory. Neuroscience. 139 (1):173–180.
DeSouza JF, Dukelow SP, Gati JS, Menon RS, Andersen RA, Vilis T. 2000. Eye position signal modulates a human parietal pointing region during memory-guided movements. J Neurosci. 20:5835–5840.
Engel SA, Glover GH, Wandell BA. 1997. Retinotopic organization in human visual cortex and the spatial precision of functional MRI. Cereb Cortex. 7:181–192.
Fabbri S, Caramazza A, Lingnau A. 2012. Distributed sensitivity for movement amplitude in directionally tuned neuronal populations. J Neurophysiol. 107:1845–1856.
Farrer C, Frey SH, Van Horn JD, Tunik E, Turk D, Inati S, Grafton ST. 2008. The angular gyrus computes action awareness representations. Cereb Cortex. 18 (2):254–61.
Fernandez-Ruiz J, Goltz HC, DeSouza JFX, Vilis T, Crawford JD. 2007. Human parietal "reach region" primarily encodes intrinsic visual direction, not extrinsic movement direction, in a visual motor dissociation task. Cereb Cortex. 17: 2283–2292.
Filimon F, Nelson JD, Huang R-S, Sereno MI. 2009. Multiple parietal reach regions in humans: cortical representations for visual and proprioceptive feedback during on-line reaching. J Neurosci. 29:2961–2971.
Flanagan JR, Johansson RS. 2003. Action plans used in action observation. Nature. 424:769–771.
Forman SD, Cohen JD, Fitzgerald M, Eddy WF, Mintun MA, Noll DC. 1995. Improved assessment of significant activation in functional magnetic resonance imaging (fMRI): use of a cluster-size threshold. Magn Reson Med. 33:636–647.
Gail A, Andersen RA. 2006. Neural dynamics in monkey parietal reach region reflect context-specific sensorimotor transformations. J Neurosci. 26:9376–9384.
Gail A, Klaes C, Westendorff S. 2009. Implementation of spatial transformation rules for goal-directed reaching via gain modulation in monkey parietal and premotor cortex. J Neurosci. 29 (30):9490–9499.
Gallivan JP, Cavina-Pratesi C, Culham JC. 2009. Is that within reach? fMRI reveals that the human superior parieto-occipital cortex encodes objects reachable by the hand. J Neurosci. 29:4381–4391.
Gallivan JP, Culham JC. 2015. Neural coding within human brain areas involved in actions. Curr Opin Neurobiol. 33:141–149.
Gallivan JP, McLean A, Culham JC. 2011. Neuroimaging reveals enhanced activation in a reach-selective brain area for objects located within participants' typical hand workspaces. Neuropsychologia. 49:3710–3721.
Gertz H, Fiehler K. 2015. Human posterior parietal cortex encodes the movement goal in a pro-/anti-reach task. J Neurophysiol. 114:170–183.
Gu C, Wood DK, Gribble PL, Corneil BD. 2016. A trial-by-trial window into sensorimotor transformations in the human motor periphery. J Neurosci. 36 (31):8273–8282.
Gutteling TP, Petridou N, Dumoulin SO, Harvey BM, Aarnoutse EJ, Kenemans JL, Neggers SF. 2015. Action preparation shapes processing in early visual cortex. J Neurosci. 35 (16): 6472–6480.
Henriques DY, Klier EM, Smith MA, Lowy D, Crawford JD. 1998. Gaze-centered remapping of remembered visual space in an open-loop pointing task. J Neurosci. 18:1583–1594.
Hirnstein M, Bayer U, Ellison A, Hausmann M. 2011. TMS over the left angular gyrus impairs the ability to discriminate left from right. Neuropsychologia. 49 (1):29–33.
Jerde TA, Merriam EP, Riggall AC, Hedges JH, Curtis CE. 2012. Prioritized maps of space in human frontoparietal cortex. J Neurosci. 32 (48):17382–90.
Khan AZ, Crawford JD, Blohm G, Urquizar C, Rossetti Y, Pisella L. 2007. Influence of initial hand and target position on reach errors in optic ataxic and normal subjects. J Vis. 7:81–16.
Konen CS, Mruczek REB, Montoya JL, Kastner S. 2013. Functional organization of human posterior parietal cortex: grasping- and reaching-related activations relative to topographically organized cortex. J Neurophysiol. 109:2897–2908.
Kravitz DJ, Saleem KS, Baker CI, Mishkin M. 2011. A new neural framework for visuospatial processing. Nat Rev Neurosci. 12 (4):217–230.
Kuang S, Morel P, Gail A. 2016. Planning movements in visual and physical space in monkey posterior parietal cortex. Cereb Cortex. 26 (2):731–747.
Lauritzen TZ, D'Esposito M, Heeger DJ, Silver MA. 2009. Top-down flow of visual spatial attention signals from parietal to occipital cortex. J Vis. 9 (13):18.
Makino Y, Yokosawa K, Takeda Y, Kumada T. 2004. Visual search and memory search engage extensive overlapping cerebral cortices: an fMRI study. Neuroimage. 23:525–533.
Malik P, Dessing JC, Crawford JD. 2015. Role of early visual cortex in trans-saccadic memory of object features. J Vis. 15 (11):7.
Medendorp WP, Goltz HC, Crawford JD, Vilis T. 2005. Integration of target and effector information in human posterior parietal cortex for the planning of action. J Neurophysiol. 93: 954–962.

Medendorp WP, Goltz HC, Vilis T, Crawford JD. 2003. Gaze-centered updating of visual space in human parietal cortex. J Neurosci. 23:6209–6214.

Messier J, Kalaska JF. 2000. Covariation of primate dorsal premotor cell activity with direction and amplitude during a memorized-delay reaching task. J Neurophysiol. 84 (1): 152–165.

Monaco S, Cavina-Pratesi C, Sedda A, Fattori P, Galletti C, Culham JC. 2011. Functional magnetic resonance adaptation reveals the involvement of the dorsomedial stream in hand orientation for grasping. J Neurophysiol. 106: 2248–2263.

Pasternak T, Greenlee MW. 2005. Working memory in primate sensory systems. Nat Rev Neurosci. 6:97–107.

Perenin MT, Vighetto A. 1988. Optic ataxia: a specific disruption in visuomotor mechanisms. I. Different aspects of the deficit in reaching for objects. Brain. 111 (Pt 3):643–674.

Perry CJ, Sergio LE, Crawford JD, Fallah M. 2015. Hand placement near the visual stimulus improves orientation selectivity in V2 neurons. J Neurophysiol. 113 (7):2859–2870.

Picard N, Strick PL. 2001. Imaging the premotor areas. Curr Opin Neurobiol. 11:663–672.

Prado J, Clavagnier S, Otzenberger H, Scheiber C, Kennedy H, Perenin M-T. 2005. Two cortical systems for reaching in central and peripheral vision. Neuron. 48:849–858.

Pratte MS, Tong F. 2014. Spatial specificity of working memory representations in the early visual cortex. J Vis. 14 (3):22.

Rawley JB, Constantinidis C. 2009. Neural correlates of learning and working memory in the primate posterior parietal cortex. Neurobiol Learn Mem. 91:129–138.

Rizzolatti G, Riggio L, Dascola I, Umiltá C. 1987. Reorienting attention across the horizontal and vertical meridians: evidence in favor of a premotor theory of attention. Neuropsychologia. 25:31–40.

Rolfs M, Lawrence B, Carrasco M. 2013. Reach preparation enhances visual performance and appearance. Philos Trans R Soc B Biol Sci. 368:20130057.

Rossetti Y, Pisella L, Vighetto A. 2003. Optic ataxia revisited: visually guided action versus immediate visuomotor control. Exp Brain Res. 153 (2):171–179.

Sadeh M, Sajad A, Wang H, Yan X, Crawford JD. 2015. Spatial transformations between superior colliculus visual and motor response fields during head-unrestrained gaze shifts. Eur J Neurosci. 42 (11):2934–51.

Sajad A, Sadeh M, Keith GP, Yan X, Wang H, Crawford JD. 2015. Visual-Motor transformations within frontal eye fields during head-unrestrained gaze shifts in the monkey. Cereb Cortex. 25 (10):3932–52.

Sajad A, Sadeh M, Yan X, Wang H, Crawford JD. 2016. Transition from target to gaze coding in primate frontal eye field during memory delay and memory–motor transformation. eNeuro. 3 (2):1–20e0040-16.2016.

Singh KD, Smith AT, Greenlee MW. 2000. Spatiotemporal frequency and direction sensitivities of human visual areas measured using fMRI. Neuroimage. 12:550–564.

Singhal A, Monaco S, Kaufman LD, Culham JC. 2013. Human fMRI reveals that delayed action re-recruits visual perception. PLoS One. 8 (9):e73629.

Snyder LH. 2000. Coordinate transformations for eye and arm movements in the brain. Curr Opin Neurobiol. 10:747–754.

Srimal R, Curtis CE. 2008. Persistent neural activity during the maintenance of spatial position in working memory. Neuroimage. 39 (1):455–468.

Tosoni A, Galati G, Romani GL, Corbetta M. 2008. Sensory-motor mechanisms in human parietal cortex underlie arbitrary visual decisions. Nat Neurosci. 11:1446–1453.

Uchimura M, Nakano T, Morito Y, Ando H, Kitazawa S. 2015. Automatic representation of a visual stimulus relative to a background in the right precuneus. Eur J Neurosci. 42 (1):1651–1659.

Van Der Werf J, Jensen O, Fries P, Medendorp WP. 2008. Gamma-band activity in human posterior parietal cortex encodes the motor goal during delayed prosaccades and antisaccades. J Neurosci. 28 (34):8397–8405.

Van Der Werf J, Jensen O, Fries P, Medendorp WP. 2010. Neuronal synchronization in human posterior parietal cortex during reach planning. J Neurosci. 30 (4):1402–1412.

Vesia M, Crawford JD. 2012. Specialization of reach function in human posterior parietal cortex. Exp Brain Res. 221:1–18.

Vesia M, Monteon JA, Sergio LE, Crawford JD. 2006. Hemispheric asymmetry in memory-guided pointing during single-pulse transcranial magnetic stimulation of human parietal cortex. J Neurophysiol. 96 (6):3016–3027.

Vesia M, Prime SL, Yan X, Sergio LE, Crawford JD. 2010. Specificity of human parietal saccade and reach regions during transcranial magnetic stimulation. J Neurosci. 30: 13053–13065.

Weinrich M, Wise SP. 1982. The premotor cortex of the monkey. J Neurosci. 2 (9):1329–1345.

Westendorff S, Klaes C, Gail A. 2010. The cortical timeline for deciding on reach motor goals. J Neurosci. 30:5426–5436.

Zhang M, Barash S. 2000. Neuronal switching of sensorimotor transformations for antisaccades. Nature. 408 (6815):971–975.